


Hybrid QM/classical models: Methodological advances and new applications

Cite as: Chem. Phys. Rev. 2, 041303 (2021); <https://doi.org/10.1063/5.0064075>

Submitted: 20 July 2021 • Accepted: 01 October 2021 • Published Online: 27 October 2021

 Filippo Lipparini and  Benedetta Mennucci

COLLECTIONS

 This paper was selected as Featured



View Online



Export Citation



CrossMark



Applied Physics
Reviews

Read. Cite. Publish. Repeat.

19.162
2020 IMPACT FACTOR*



Hybrid QM/classical models: Methodological advances and new applications

Cite as: Chem. Phys. Rev. **2**, 041303 (2021); doi: [10.1063/5.0064075](https://doi.org/10.1063/5.0064075)

Submitted: 20 July 2021 · Accepted: 1 October 2021 ·

Published Online: 27 October 2021





View Online



Export Citation



CrossMark

Filippo Lipparini^{a)}  and Benedetta Mennucci^{b)} 

AFFILIATIONS

Dipartimento di Chimica e Chimica Industriale, University of Pisa, Via G. Moruzzi 13, 56126 Pisa, Italy

^{a)}Electronic mail: filippo.lipparini@unipi.it

^{b)}Author to whom correspondence should be addressed: benedetta.mennucci@unipi.it

ABSTRACT

Hybrid methods that combine quantum mechanical descriptions with classical models are very popular in molecular modeling. Such a large diffusion reflects their effectiveness, which over the years has allowed the quantum mechanical description to extend its boundaries to systems of increasing size and to processes of increasing complexity. Despite this success, research in this field is still very active and a number of advances have been made recently, further extending the range of their applications. In this review, we describe such advances and discuss how hybrid methods may continue to improve in the future. The various formulations proposed so far are presented here in a coherent way to underline their common methodological aspects. At the same time, the specificities of the different classical models and of their coupling with the quantum mechanical domain are highlighted and discussed, with special attention to the computational and numerical aspects.

© 2021 Author(s). All article content, except where otherwise noted, is licensed under a Creative Commons Attribution (CC BY) license (<http://creativecommons.org/licenses/by/4.0/>). <https://doi.org/10.1063/5.0064075>

TABLE OF CONTENTS

I. INTRODUCTION	1
II. CONTINUUM AND ATOMISTIC FORMULATIONS	2
A. Continuum solvation models	3
B. QM/MM models	4
C. Three-layer models	5
D. Linear scaling implementations	6
E. Nonelectrostatic interactions	7
III. PRESENT AND FUTURE APPLICATIONS	8
A. From energies to spectroscopies and dynamics	8
B. From solvents and biomatrices to composite systems	10
IV. OUTLOOK	11
ACKNOWLEDGMENTS	12
DATA AVAILABILITY	12

I. INTRODUCTION

More than 40 years ago, different research groups had the same revolutionary idea of combining quantum chemistry with models developed in classical physics.^{1–3} The idea was developed along two alternative lines: one maintained an atomistic description of the classical subsystem while the other shifted to an implicit or continuum description.

In their very first formulations, the atomistic methods focused on biosystems while the continuum ones focused on solvated molecules. The reasons for this differentiation are clear. A continuum description works well when the effects of the environment can be properly approximated as a mean field, i.e., for environments that are homogeneous and fast in their configurational dynamics and do not present strong and persistent specific interactions with the quantum-mechanical (QM) subsystem. All these aspects are valid for many of the most common solvents but surely they are less applicable to biological matrices that instead can be properly described in terms of classical but atomistic models, e.g., molecular mechanics (MM) force fields. In addition to the preferential fields of application, the two alternative strategies also diversified in terms of the property/process they were applied to. Since the very beginning, the most natural application of continuum models was the evaluation of thermodynamic properties, such as solvation-free energies,^{4–6} while atomistic approaches were mostly used in the field of (bio)reactivity and, in particular, enzymatic processes.^{7–10}

The resulting hybrid strategies are nowadays known as continuum solvation models and QM/MM, respectively.

In the last few decades, both strategies have been reformulated and extended in many different ways and are now the most popular approaches to describe the properties and processes of molecular

systems embedded in an environment. Over the years, the initial diversity of applications of the two formulations has been largely softened, and today they can be alternatively used or even combined to describe a large set of problems, ranging from the prediction of spectroscopies^{11,12} to the simulation of ground and excited state (nonadiabatic) dynamics of molecules in solutions and in more complex matrices,^{13,14} to the study of photo-induced phenomena in biosystems and artificial (bio)nanostructures.^{15–17} All this has been made possible by the many important advances that have been introduced in their theoretical and computational aspects. The focus of this review is mostly on these advances and is organized in two main sections. In Sec. II, we describe the main methodological aspects of the different formulations of QM/classical approaches. Next, in Sec. III, we focus on the main recent applications of the same methods discussing the methodological advances that have allowed them. We conclude by presenting an outlook in Sec. IV on the future directions that we think will allow hybrid methods to continue to play a fundamental role in the modeling of complex systems for many years.

II. CONTINUUM AND ATOMISTIC FORMULATIONS

In this section, we briefly describe the various formulations of atomistic and continuum models that are currently used in combination with a QM description for modeling environment effects.

In general, both atomistic and continuum models describe environment effects on the QM subsystem through an electrostatic charge density, which can be permanent (M) or induced (X) or both. If an induced density is present, the model is said to be polarizable. From a physical point of view, this is a very attractive feature, as it allows the environment to adapt to the QM density and to respond to its changes, making the model, in general, more flexible. Assuming that the polarizable model is linear, the polarization density X is determined by solving a linear equation $AX = -\Theta(\rho, M)$ where A is a model-dependent polarization matrix and Θ is a linear function of the classical permanent density M and the QM one (ρ). A final ingredient that is needed to define the model is an expression for the polarization energy. This is usually the Coulomb interaction between X , M , and ρ , but it can also be a slightly modified version thereof, e.g., to exclude interactions between bonded atoms or to avoid overpolarization if two atoms get too close. We assume anyways that the energy expression can be written as $E_{\text{pol}} = 1/2 \langle X, \Psi(\rho, M) \rangle$, where $\Psi(\rho, M)$ is a (linear) function of the QM and permanent charge densities. The notation $\langle a, b \rangle$ denotes a scalar product in the appropriate vector space. To avoid lengthy mathematical discussions, we assume that the models have been discretized, i.e., that the permanent and polarization densities are represented with a finite collection of variables, so that the vector space we work in is always \mathbb{R}^n .

While polarizable models are a well-established tool in computational chemistry, having been available for more than three decades, there are many subtleties in their formulation that can complicate the derivation of the various coupled equations, especially when analytical derivatives are required. For this reason, we have recently introduced a completely general Lagrangian formalism¹⁸ that can not only be used for any (linear) polarizable model but also make the calculation of analytical derivatives and coupled QM/embedding equations straightforward. In such a formalism, the embedded system is described by the following Lagrangian:

$$\mathcal{G}(\rho, X; M) = E^{\text{QM}}(\rho) + E^{\text{self}}(M) + \langle \Phi(\rho), M \rangle + \frac{1}{2} \langle X, \Psi(\rho, M) \rangle + \frac{1}{2} \langle S, AX + \Theta(\rho, M) \rangle. \quad (1)$$

The Lagrangian in Eq. (1) is given by the sum of the QM energy $E^{\text{QM}}(\rho)$; the self-interaction energy of the permanent charge distribution $E^{\text{self}}(M)$; the interaction energy between ρ and M $\langle \Phi(\rho), M \rangle$, where $\Phi(\rho)$ is an appropriate linear function of the QM density; and the polarization energy. The last term is a constraint that, using the Lagrange multiplier S , enforces the polarization equations. As it will be shown in Secs. II A and II B, the specific definition of all the aforementioned quantities depends on the model.

In the following, we assume that the polarization model is linear, i.e., that the induced density X is obtained by solving a linear equation. The most notable exception to this are solvation models based on the Poisson–Boltzmann equation, which we briefly discuss in Sec. II A.

In general, we can write the functions Φ , Ψ , and Θ as a density-independent term due to the nuclei and to M plus the contraction of the appropriate one-electron integrals with the density, i.e.,

$$\Phi(\rho, M) = \Phi(M) + \Phi^{\text{nuc}}(Z) + \sum_{\mu\nu} P_{\mu\nu} \Phi_{\mu\nu}, \quad (2)$$

where we have introduced a basis of atomic orbitals χ_{μ} , $\mu = 1, N_b$ and P is the corresponding density matrix. Analogous expressions are used for the other quantities.

If a self-consistent field (SCF) level of theory—such as Hartree–Fock (HF) or Kohn–Sham density functional theory (DFT)—is used, the Fock or Kohn–Sham matrix that defines the Roothaan equations is obtained by differentiating the Lagrangian in Eq. (1) with respect to the density matrix as follows:

$$F_{\mu\nu}(P) = F_{\mu\nu}^{\text{QM}}(P) + \langle \Phi_{\mu\nu}, M \rangle + \frac{1}{2} \langle \Psi_{\mu\nu}, X \rangle + \frac{1}{2} \langle \Theta_{\mu\nu}, S \rangle. \quad (3)$$

The polarization and Lagrange multiplier equations are obtained by differentiating the Lagrangian with respect to S and X , respectively. Thus,

$$AX = -\Theta(\rho, M); \quad A^\dagger S = -\Psi(\rho, M). \quad (4)$$

We note here that for nonpolarizable models, the terms involving X and S vanish and there are no polarization equations to solve. Furthermore, many polarizable models are variational, i.e., A is symmetric and positive definite. For variational models, $X = S$ and the equations simplify. Various examples are given in Secs. II A and II B.

Embedded calculations going beyond HF or DFT require some further considerations. If the embedding is not polarizable, the calculations can be performed exactly as *in vacuo*, but with a modified one-electron Hamiltonian that includes the $\langle \Phi_{\mu\nu}, M \rangle$ contribution. Things are more complicated when a polarizable embedding model is introduced, as the polarization introduces a density-dependent term into the molecular Hamiltonian. Many different strategies have been presented to couple a post-HF level of theory with a polarizable method.^{19–31} The various strategies can be grouped into three families.¹⁹ In perturbation to the energy (PTE) methods, the polarizable embedding is used to solve the SCF problem in a self-consistent fashion, while the post-HF amplitudes are obtained ignoring the polarization. In perturbation to the density (PTD) methods, the correlated density computed without polarization is used to evaluate the response

of the environment. Finally, in perturbation to the energy and density (PTED) methods, an iterative solution to the amplitude equations is obtained, to achieve full mutual polarization. The latter strategy sounds in principle more attractive but is very expensive and suffers from some theoretical inconsistencies.²⁰ Substantially cheaper, yet accurate, approximations to the PTED scheme have also been developed.²⁸

A. Continuum solvation models

In continuum formulations of the QM/classical approach, the classical subsystem is represented as an infinite dielectric of permittivity $\varepsilon(r)$ while the QM subsystem is assumed to be accommodated in a molecular cavity Ω within the dielectric medium. In its more general formulation, an average density of ionic species is also considered, and the electrostatic potential of the embedded system satisfies the following Poisson's equation:

$$\nabla \cdot (\varepsilon(r) \nabla \phi) = 4\pi(\rho + \rho^{\text{ions}}), \quad (5)$$

where ρ^{ions} is the density of ions and $\varepsilon(r)$ is a function of the position. The latter dependence is connected to the definition of the molecular cavity.

As ρ^{ions} is in general not known, a model needs to be adopted. The most common choice is to assume that the ions follow a Boltzmann distribution as follows:

$$\rho^{\text{ions}}(r) = \lambda(r) \sum_{i=1}^M q_i c_i^b \exp\left(-\frac{q_i \phi(r)}{k_B T}\right), \quad (6)$$

where $\lambda(r)$ is an exclusion function that ensures that the concentration of ions goes to zero inside the molecular cavity, the sum runs over all the electrolytes, and c_i^b q_i are the bulk concentration and charge of the i th electrolyte, respectively. By plugging Eq. (6) into (5), the nonlinear Poisson–Boltzmann equation (PBE) is obtained. Solvation models based on PBE have the nontrivial problem of solving a nonlinear partial differential equation, and require advanced numerical strategies.^{32–38}

In most continuum solvation models, typically used in quantum chemistry, the cavity is defined as a sharp interface and the position dependency of $\varepsilon(r)$ is simplified as follows:

$$\varepsilon(r) = \begin{cases} 1, & r \in \Omega, \\ \varepsilon_s, & r \in \mathbb{R}^3 \setminus \Omega, \end{cases} \quad (7)$$

where ε is the bulk permittivity of the solvent. Within this approximation, the electrostatic problem can easily be recast as an integral equation on the cavity's boundary by introducing an *apparent surface charge* (ASC). ASC formulations are efficient, versatile, and easier to implement, to the point that the vast majority of quantum chemistry packages offer some solvation model based on an ASC formulation.

ASC formulations were originally introduced for nonionic solutions, for which the general Poisson equation holds, i.e.,

$$\nabla \cdot (\varepsilon(r) \nabla \phi) = 4\pi\rho. \quad (8)$$

At the boundary of the cavity $\Gamma = \partial\Omega$, the potential ϕ presents a discontinuity in the normal derivative, which has the physical meaning of an induced surface charge σ . The solution ϕ can be obtained as a sum of the potential of ρ^{QM} *in vacuo* (Φ) and the so-called *reaction*

potential W accounting for the polarization effects of the environment. As Φ is continuous with continuous normal derivative across Γ , we get

$$\sigma(s) = \frac{1}{4\pi} \left[\frac{\partial W}{\partial n} \right] (s), \quad (9)$$

where we denote the jump (inside minus outside) with square brackets. ASC formulations of continuum models transform the three-dimensional Poisson partial differential equation into a two-dimensional integral equation on Γ , that has the general form

$$\mathcal{T}\sigma = -\mathcal{R}\Phi, \quad (10)$$

where \mathcal{T} and \mathcal{R} are operators on $L^2(\Gamma)$, with \mathcal{T} being positive and self-adjoint. The two most commonly used ASC continuum models are the integral equation formalism polarizable continuum model³⁹ (IEF-PCM), which has become the *de facto* standard in the PCM family of models to the point that it is usually referred to simply as PCM, and the conductor-like screening model^{6,40} (COSMO). COSMO, which has been also reformulated within the PCM framework and it is known as C-PCM,⁴¹ approximates the dielectric solvent with a conductor and then introduces an empirical scaling to recover the correct dielectric response. The integral equation for IEF-PCM reads

$$\left(2\pi \frac{\varepsilon + 1}{\varepsilon - 1} - \mathcal{D} \right) \mathcal{S}\sigma = -(2\pi - \mathcal{D})\Phi, \quad (11)$$

where

$$\mathcal{S}\sigma = \int_{\Gamma} ds' \frac{\sigma(s')}{|s - s'|}, \quad \mathcal{D}\sigma = \int_{\Gamma} ds' \sigma(s') \frac{\partial}{\partial n_s} \frac{1}{|s - s'|}.$$

We note that the IEF-PCM model is equivalent to the SS(V)PE model by Chipman.⁴² The solvation energy is then obtained as half the electrostatic interaction energy between σ and the solute's potential as follows:

$$E_s = \frac{1}{2} \int_{\Gamma} ds \sigma(s) \Phi(s). \quad (12)$$

The IEF-PCM method is not limited to the treatment of standard, isotropic, nonionic solution and has been formulated also for anisotropic and weakly ionic solvents, the latter formulation being based on the linearized PBE.⁴³

The COSMO equation is obtained in the framework of a conductor instead of a dielectric; as such, it can be seen as the limit for an infinite dielectric constant of the IEF-PCM equation as follows:

$$\mathcal{S}\sigma = -\Phi, \quad (13)$$

and the COSMO solvation energy is

$$E_s = \frac{1}{2} f(\varepsilon) \int_{\Gamma} ds \sigma(s) \Phi(s), \quad (14)$$

where $f(\varepsilon)$ is an empirical scaling function used to recover the dielectric behavior.

The solution to the COSMO and IEF-PCM equations is nontrivial for general molecule-shaped cavities and is obtained numerically by discretizing the integral equations by introducing a mesh of the surface cavity.^{44,45} Alternatively, a discretization of σ can be obtained using a

basis of spherical Gaussians placed at representative points on the surface cavity. The latter method, originally introduced by York and Karplus for COSMO,⁴⁶ has been extended to the PCM family of models by Scalmani and Frisch⁴⁷ and, independently, by Lange and Herbert,^{48,49} and it has become the standard for the numerical implementation of ASC methods. Independent of the discretization, the ASC is replaced by a collection of charges q and the integral operators by their matrix representation. Before discussing how to use the formalism presented in Sec. II, an important technical note is mandatory. While the integral operator that defines the IEF-PCM is self-adjoint, its matrix representation is, in general, not. In other words, while the model in its continuous formulation is variational, its practical realization loses this property due to numerical issues.⁵⁰ A variational formulation is possible if the equation is symmetrized *a posteriori*, by replacing the discretized \mathcal{S} operator with $\frac{1}{2}(\mathcal{S} + \mathcal{S}^\dagger)$, which allows for a genuine variational formulation of PCM⁵¹ at the price of some implementation complications. As an alternative, the Lagrangian formalism of Sec. II can be used as follows:

$$\mathcal{G}(\rho, q, w) = E^{\text{QM}}(\rho) + \frac{1}{2}\langle q, V \rangle + \frac{1}{2}\langle w, Tq + RV \rangle, \quad (15)$$

where T and R are matrix representations of the suitable integral operators, V is the discretized electrostatic potential at the cavity points, w are Lagrange multipliers, and q are the discretization coefficients of the ASC. COSMO does not suffer from discretization-related issues, as the matrix representation S of the \mathcal{S} operator is symmetric. Therefore, the COSMO free energy functional is given by

$$\mathcal{G}(\rho, q) = \frac{1}{2}f(\varepsilon)\langle q, Sq \rangle + f(\varepsilon)\langle q, V \rangle. \quad (16)$$

We conclude this section by recalling that alternative strategies to the ASC have been proposed. One of these strategies uses a smooth interface redefining the permittivity as a smooth self-consistent function of the QM density that interpolates between 1 and its bulk value. The so-called self-consistent continuum solvation (SCCS) model was originally formulated by Fattebert and Gygi⁵² and successively reformulated in a more general and effective way by Andreussi and co-workers.^{32,36} The SCCS model has been designed for first-principles molecular dynamics (MD) simulations, plane wave basis sets, and periodic boundary conditions. A further approximate yet effective alternative is the so-called generalized Born model (GB).⁵³ From a computational point of view, GB methods are vastly simpler and faster than the ASC formulations, to the point that GB methods are the standard solvation models for classical descriptions of macromolecular systems and their dynamics. Their use in quantum chemistry is more limited, the only notable exception being the SM-X family of solvation models⁴ developed by Cramer and Truhlar and co-workers.

B. QM/MM models

As seen for continuum models, also when atomistic classical models are used in combination with a QM description, different formulations are possible: within this context they are called embeddings.

The most common embedding model is the *electrostatic embedding* (EE) approach, where the classical atoms bear a point charge that is allowed to interact with the QM density. EE has the advantage of

being simple and inexpensive, while at the same time being able to properly describe directional, specific interactions such as hydrogen bonding. Using the notation introduced in Sec. II, a point charge-based embedding can be represented by dropping the last two terms of Eq. (1), obtaining the following energy functional:

$$\mathcal{G}(\rho; q) = E^{\text{QM}}(\rho) + E^{\text{self}}(q) + \langle \Phi(\rho), q \rangle, \quad (17)$$

where, denoting the point charges by q_i and their positions by r_i ,

$$E^{\text{self}}(q) = \frac{1}{2} \sum_{i \neq j} \frac{q_i q_j}{|r_i - r_j|}, \quad (18)$$

$$\Phi_i(\rho) = \sum_{\alpha} \frac{Z_{\alpha}}{|r_{\alpha} - r_i|} - \sum_{\mu\nu} P_{\mu\nu} \int_{\mathbb{R}^3} \frac{\chi_{\mu}(r) \chi_{\nu}(r)}{|r - r_i|} d^3 r, \quad (19)$$

and where $\langle \Phi(\rho), q \rangle = \sum_i q_i \Phi_i(\rho)$. Note that the dependence of the energy on the point charges is parametric; as a consequence, the contribution of the MM region to the QM energy is limited to an additional electrostatic term in the one-electron interactions plus the classical electrostatic interaction between all the classical charges (q and Z). It is important to mention that a simple electrostatic picture based on distributed point charges may not be enough to provide an accurate representation of the electrostatics of the environment. The use of higher order multipoles, such as dipoles and quadrupoles, can consistently improve such a picture, especially for small solvent molecules,^{54–56} while point charges can be sufficient for large, biological matrices.⁵⁷ The reader is referred to the literature for a more detailed analysis of the importance of higher order electrostatic representations.^{55–57}

A description of the environment in an EE model is intrinsically static, as the electric field generated by the environment only depends on the positions of the MM atoms, with the atomic charges being fixed. In other words, while the MM environment polarizes the QM solute, the contrary is not true. Polarizable embeddings (PEs) overcome this limitation by allowing the electrostatic distribution of the environment to respond to an external field.^{58–61} In PE models, the permanent electrostatic distribution M is either augmented or replaced with an additional polarizable one X , giving rise to the complete energy functional in Eq. (1).

Several models have been proposed for the polarization. In the fluctuating charges (FQ) model,^{62–64} the environment bears charges q that respond to differences in parametrized atomic electronegativities χ and changes in the electrostatic potential Φ , under the constraint that every fragment α (e.g., solvent molecule) has a fixed total charge Q_{α} as follows:

$$\begin{cases} Jq = -\chi - \Phi(\rho), \\ \sum_{i \in \alpha} q_i = Q_{\alpha}. \end{cases} \quad (20)$$

The constraint can be enforced with a set of Lagrange multipliers λ , leading to the energy functional

$$\begin{aligned} \mathcal{G}(\rho, q, \lambda) = & E^{\text{QM}}(\rho) + \langle q, \Phi(\rho) \rangle + \frac{1}{2} \langle q, Jq \rangle \\ & + \sum_{\alpha} \lambda_{\alpha} \left(\sum_{i \in \alpha} q_i - Q_{\alpha} \right). \end{aligned} \quad (21)$$

The FQ model is variational and has been extensively developed and used to describe properties and spectroscopies of molecules in water.^{65,66}

The induced point dipole (IPD) model^{67–75} introduces the environment polarization as a linear response to an inducing field, by endowing each MM atom with a polarizability. The inducing field E is produced by both the permanent electrostatic distribution M of the MM atoms and the QM density, according to the equation

$$T\mu = E(\rho, M), \quad (22)$$

where the matrix T has inverse polarizability tensors on its diagonal and dipole–dipole interaction tensors between sites i and j on its off-diagonal blocks. For a model including point charges and induced dipoles, the energy functional reads

$$\mathcal{G}(\rho, \mu; q) = E^{\text{QM}}(\rho) + \langle q, \Phi(\rho) \rangle + E^{\text{self}}(q) + \frac{1}{2} \langle \mu, T\mu \rangle - \langle \mu, E(\rho, q) \rangle, \quad (23)$$

where

$$E_i(\rho, q) = \sum_{\alpha} Z_{\alpha} \frac{r_{\alpha} - r_i}{|r_{\alpha} - r_i|^3} - \sum_{\mu\nu} P_{\mu\nu} \int_{\mathbb{R}^3} \chi_{\mu}(r) \chi_{\nu}(r) \frac{r - r_i}{|r - r_i|^3} d^3r + \sum_{k \neq i} q_k \frac{r_k - r_i}{|r_k - r_i|^3}, \quad (24)$$

and the k sum runs over the MM sites.

Among the different IPD formulations proposed so far, it is worth mentioning the one based on the use of the AMOEBA force field (FF).⁷⁶ The latter in fact represents one of the most advanced and general polarizable FFs. Within the AMOEBA framework, the electrostatic interactions are described through an accurate multipolar expansion up to quadrupoles whereas polarization is represented by induced dipoles. However, a peculiarity of AMOEBA is that the polarization energy is not variational in the induced dipoles. In fact, the energy is computed as the interaction of induced dipoles with a MM electric field, which is different from the field responsible for inducing the dipoles themselves. As a consequence, the energy functional in Eq. (23) is not suited for the AMOEBA force field, and a more general Lagrangian formulation needs to be employed as follows:

$$\mathcal{G}(\rho, \mu_p, \mu_d; M) = E^{\text{QM}}(\rho) + \langle M, \Phi(\rho) \rangle + E^{\text{self}}(M) - \frac{1}{2} \langle \mu_d, E_p(\rho, M) \rangle + \frac{1}{2} \langle \mu_p, T\mu_d - E_d(\rho, M) \rangle. \quad (25)$$

Using the Lagrangian in Eq. (25), the coupled QM/AMOEBA equations are easily derived as seen in the general case. The derivation of analytical gradients, for both ground and excited state QM systems, can also be achieved using the same tools.^{18,77,78}

A third polarization model is the Drude oscillator (DO) method,^{79–84} where each atom is associated with an auxiliary particle of charge q_i , attached to the atom with a spring with force constant k_i . The action of an external electric field displaces the charge from its equilibrium position, the new position being

$$d_i = \frac{q_i E_i}{k_i}. \quad (26)$$

The off-center charge then creates an induced dipole

$$\mu_i = q_i d_i = \frac{q_i^2}{k_i} E_i, \quad (27)$$

where the quantity q_i^2/k_i can be seen as an atomic polarizability. As a consequence, the DO model is formally equivalent to the IPD model, and a similar set of equations can be derived.

A different strategy to introduce polarization but avoiding the introduction of parameterized force fields relies on QM-based potentials obtained within a fragmentation method.⁸⁵ Very popular examples are the frozen-density embedding method^{86,87} (FDE) or the closely related subsystem DFT method,⁸⁸ the effective fragment potential (EFP) method,^{89,90} and the explicit polarization model (X-Pol).⁹¹ In XPol, each fragment is treated at the QM level in a field of point charges that represent electrostatic interactions with the other fragments. To account for many-body polarization, the charges are updated self-consistently by approximating each fragment's electron density onto atom-centered point charges. The XPol can be augmented with empirical, Lennard-Jones-type intermolecular potentials in order to account for nonelectrostatic interactions. EFP can be combined with QM methods in a QM/MM fashion, providing polarizable embedding for the description of chemical and photochemical phenomena in condensed phases. The electrostatic term is based on a multipole expansion, up to octopoles computed at atom and bond midpoints. For polarization, an IPD formulation is used. The induced dipoles originate at the centroids of localized molecular orbitals (LMOs), where the (anisotropic) distributed polarizability tensors are placed. The EFP terms are parameterized; but in contrast to classical force fields, the parameters are obtained from a set of QM calculations on a gas-phase fragment. Finally, the FDE and related methods are a completely different, and intrinsically quantum-mechanical, strategy to solve the DFT equations of complex systems by introducing a fragmentation and describing each fragment in the embedding potential produced by the others, possibly by self-consistently adjusting the potential itself. As a detailed discussion of these methods is far beyond the scope of this work, the interested reader is referred to a recent review⁸⁷ for the details of this method.

We conclude this section with an important remark. In QM/MM methods, the partition of systems may not be obvious when the quantum and the classical subsystems are covalently bonded. Furthermore, the cleavage of a bond can in principle introduce unphysical, highly reactive electronic configurations that need to be saturated. For this purpose, several different methodologies have been developed. Such methodologies can be grouped into three main families: link-atom schemes introduce an additional atom—usually, a hydrogen atom—to saturate the valence at the boundary; pseudo-atom schemes replace the MM atom at the boundary with a special atom that, thanks to basis functions and pseudopotentials, saturates the valence of the QM subsystem while behaving as a MM atom in the MM region; and finally, localized orbitals schemes use local orbitals at the boundary, keeping some of them frozen, to cap the QM region. A detailed and exhaustive review of all the various schemes proposed in the literature can be found in Refs. 92 and 93.

C. Three-layer models

As already commented, atomistic and continuum models are two complementary approaches in the way they introduce environment

effects. In fact, the former are extremely effective at describing directional and specific short-range interactions, while the latter take care of long-range electrostatics in a statistically correct and computationally cheap way. It is therefore a natural idea to combine the strengths of the two approaches in a three-layered QM/MM/continuum one (see Fig. 1).

As a matter of fact, the coupling is straightforward when a non-polarizable force field is used for the MM region. In this case, what changes is only the continuum model as now the cavity has to be enlarged to include the MM atoms, which also act as additional nuclei in the definition of the electrostatic potential Φ of the QM region. Instead, the MM region is not affected by the continuum model.

The complexity of the coupling, instead, increases significantly for a polarizable FF. For the sake of conciseness, we only report the main equations for two variational models. The interested reader can find the general theory for any polarizable model in Ref. 18. Let M be the collective nonpolarizable electrostatic distribution, obtained as the union of the two possibly associated with the two models, and let X and Y be the polarizable densities, A and B the corresponding polarization matrices, and Ψ_1 and Ψ_2 the inducing electrostatic properties. A global, variational free energy functional can be defined as

$$\begin{aligned} \mathcal{G}_1(\rho, X; M) = & E^{\text{QM}}(\rho) + E^{\text{self}}(M) + \langle \Phi(\rho), M \rangle \\ & + \frac{1}{2} \langle X, AX \rangle + \langle X, \Psi_1 \rangle + \frac{1}{2} \langle Y, BY \rangle \\ & + \langle Y, \Psi_2 \rangle + \langle Y, \Omega X \rangle. \end{aligned} \quad (28)$$

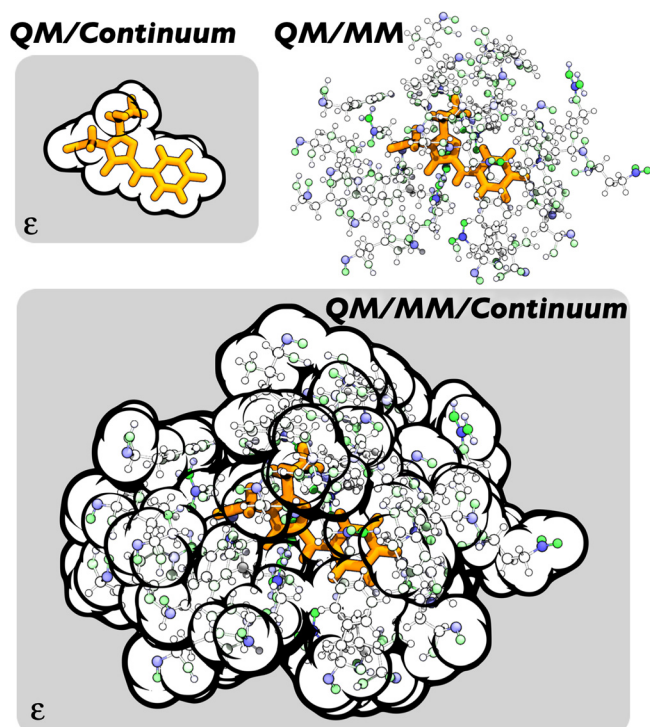


FIG. 1. Schematic representation of a continuum, a MM, and mixed MM/continuum system.

The energy functional in Eq. (28) contains the sum of the polarization contributions of each model, plus an interaction term $\langle X, \Omega Y \rangle$. The coupled polarization equations are obtained by imposing the stationarity of the global functional with respect to both polarizations and read

$$\begin{pmatrix} A & \Omega^\dagger \\ \Omega & B \end{pmatrix} \begin{pmatrix} X \\ Y \end{pmatrix} = - \begin{pmatrix} \Psi_1 \\ \Psi_2 \end{pmatrix}. \quad (29)$$

As for the single model, a nonpolarizable embedding or partially polarizable embedding (typically, a nonpolarizable MM embedding coupled with a polarizable continuum⁹⁴) can be obtained by setting the required polarization terms to zero in Eq. (28) and can be seen as a subcase of the general, polarizable setting. Contributions to the QM equations and molecular properties can be obtained using the functional in Eq. (28) as discussed in Sec. II for a single polarizable embedding.

A few fully polarizable QM/MM/continuum implementations have been proposed in the last decade. The FQ polarizable force field has been combined with the conductor screening model by Barone and co-workers.⁹⁵ The implementation, which is mainly devoted to the study of molecular response properties in solution, has been extended to analytical first and second derivatives and to the study of electric, vibrational, and magnetic response properties.^{65,66,96} Analytical gradients with respect to the position of either QM and MM nuclei are available in this implementation;⁹⁵ however, they are implemented only for a fixed, spherical molecular cavity. A three-layer, polarizable implementation based on the Drude model and on boundary potentials,^{97,98} replacing a frozen, external portion of a complex system by solving the linearized PB equation, has been successfully applied to the study of enzymatic reactions and to geometry optimizations.⁷⁹ The latter implementation is particularly well-suited for MD simulations and geometry optimization of active sites embedded in enzymes; however, to the best of our knowledge, it has not been extended to the study of molecular properties. IPD models have been successfully coupled to IEF-PCM by Steindal *et al.*⁹⁹ and, independently, by Caprasecca *et al.*,¹⁰⁰ the former implementation being specialized to (high-order) molecular properties, the latter offering analytical gradients also. More recently, Caprasecca *et al.* presented a new implementation of IPD coupled to the conductor-like screening model.¹⁰¹ The latter has been successfully used to describe the spectroscopy of complex, embedded biological systems in solutions.¹⁰²

However, fully polarizable three-layer implementations are not so commonly available, and usually present some restrictions. This is mainly due to the complexity of such implementations and to their computational cost, as the polarization equations associated with the MM and continuum model become coupled, thus increasing the computational effort associated with their solution. A larger use is however expected if new inexpensive, linear scaling formulations are implemented.

D. Linear scaling implementations

Classical embedding models are usually assumed to be an inexpensive addition to a QM computation. Due to this assumption, the development of highly efficient, linear scaling in computational cost implementations is a rather recent topic for the embedding community. Nevertheless, multiscale models have made large and very large systems accessible, which has in turn focused the attention on the

computational cost associated with embedding models. The latter problem is much more severe if a polarizable model is used.

In EE QM/MM calculations, one only needs to compute constant $[E^{\text{self}}(M)]$ energy contributions and contributions to the one-electron Hamiltonian $[\langle M, \Phi_{\mu\nu} \rangle]$, which need to be assembled once per calculation, possibly together with their derivatives. For PE models, instead, the polarization equations $AX = \Theta$ need to be solved for each value of the QM density, e.g., at each SCF cycle. The iterative solution to a large linear system, the cost of which scales with the square of the number of polarizable sites, can easily become the overall bottleneck of a calculation, surpassing even the cost associated with the QM component of the calculation itself. This problem is even more severe in continuum solvation models, where the number of polarizable sites corresponds to the number of surface elements used to mesh the cavity, and can be as large as 50–100 times the number of solvated atoms depending on the discretization. Therefore, efficient and linear scaling implementations are a necessity to extend the applicability of (polarizable) QM/classical models.

The iterative solution of the polarization equations requires one to assemble matrix-vector products, which, for a dense matrix of size N , costs $\mathcal{O}(N^2)$ floating point operations. To reduce the cost of these operations, there are two possible strategies. The most general one is to use a fast summation technique that allows the computation to be carried out in $\mathcal{O}(N)$ or $\mathcal{O}(N \log N)$ operations. As the main interaction at play in PE models is usually electrostatics, this can be achieved by using the fast multipole method (FMM).¹⁰³ FMM linear scaling implementation of continuum solvation models has been proposed by Scalmani *et al.*¹⁰⁴ and by Herbert *et al.*¹⁰⁵ Both implementations are able to handle large and very large systems with reduced effort and are well-suited for parallelization. In the context of polarizable QM/MM, a FMM-based linear scaling implementation for the MMPol IPD-based model has been proposed by one of us and generalized to arbitrary force fields and multipolar orders.¹⁰⁶ Another open-source, FMM-based linear scaling implementation of an IPD formulation of polarizable QM/MM has been recently achieved.¹⁰⁷ The availability of linear scaling polarizable QM/MM implementations has made it possible to use such strategies for performing *ab initio* MD simulations, including Born–Oppenheimer dynamics of excited states.⁷⁸

While FMM-based implementations can achieve impressive speedups for polarizable MM, allowing tens of thousands of polarizable sites to be included at little cost, even linear scaling implementations of continuum models remain expensive¹⁰⁸ when moving to very large solvated molecules. This is due to the fact that the size of the polarization matrix is usually much larger, as a relatively fine mesh is needed for the discretization of integral equations. Recently, Cancés and co-workers have proposed a different paradigm for implementing polarizable continuum solvation methods, based on the domain-decomposition (dd) technique.¹⁰⁹ An implementation of COSMO based on dd named ddCOSMO¹¹⁰ has been achieved and is available in an open-source library.^{111,112} In ddCOSMO, the polarization equations are sparse and linear scaling is naturally achieved for both the solution to the COSMO equations and the calculation of energy and forces. A dd-based implementation of the polarizable continuum model has also been proposed;¹¹³ however, it does not scale linearly in cost with respect to the system size.

Linear scaling implementations of three-layer, QM/MM/continuum models are even scarcer. An implementation for IPD coupled

with ddCOSMO has been proposed,¹⁰¹ however, without allowing analytical gradients. Nevertheless, QM/MM/continuum models are expensive, and their extension to more computationally intensive tasks, such as molecular dynamics, still requires additional efforts especially in the definition of the molecular cavity.

E. Nonelectrostatic interactions

In the methods described so far, only electrostatic and polarization interactions between the QM and the classical subsystems have been considered. These are generally the most important ones but it is a fact that a full characterization of environment effects should also include nonelectrostatic (namely, dispersion and repulsion) components.

In the context of continuum models, a very effective strategy is to introduce a simple linear relationship of the nonelectrostatic free energy and the cavity surface.^{114,115} Within this framework, the proportionality factors are either obtained by fitting procedures or derived from specific models. When a QM/MM approach is used, instead, nonelectrostatic interactions are commonly described through a Lennard-Jones type of potential, in analogy to what is done for fully classical simulations. This means that the QM subsystem is replaced by empirical parameters.

It is clear that all these formulations can only introduce a shift in the (free) energy of the system but have no effect on the QM wavefunction and the related electronic density. Attempts to go beyond this approximation have been proposed but their application is still limited mainly because these models are not yet implemented in the most diffused software and also because their theoretical foundations are less robust than for electrostatic and polarization models. We have to in fact recall that dispersion is a nonlocal electron correlation effect and that repulsion arises from the Pauli exclusion principle, namely, two purely QM effects. As a result, their reformulation within a hybrid QM/classical picture introduces much greater difficulties than electrostatics and polarization, which are well-defined also in a fully classical framework.

Within the continuum framework, an approach to include dispersion and repulsion effects directly in the effective Hamiltonian of the QM subsystem was proposed by Amovilli and Mennucci¹¹⁶ in combination with the PCM formulation of electrostatics. In short, the Pauli repulsion contribution is derived from the exchange and penetration terms of the decomposition of the intermolecular interaction energy using a simplified expression for a uniform and continuum solvent. As a result, the repulsion component of the free energy is proportional to the so-called “escaped charge,” e.g., the electronic density of the QM subsystem, which extends beyond the boundaries of the molecular cavity.

The expression for dispersion energy is instead achieved by similarity with electrostatics introducing an additional set of induced (or apparent) charges on the cavity surface. This time, the surface charges are induced by the transition densities corresponding to the excitations in the QM subsystem and they depend on the solvent refractive index measured in the visible spectrum far from the electronic transitions and the first ionization potential of the solvent. The approach has been also extended to describe solvatochromic shifts on absorption spectra.¹¹⁷ An alternative approach for including dispersion effects on solvatochromism has been proposed by Marenich *et al.*¹¹⁸ The model, known as state-specific polarizability model (SMSSP), uses two

descriptors, namely, the spherically averaged dipole polarizability of the QM subsystem (either in its ground or excited electronic state) and the refractive index of the solvent.

When the classical part is described atomistically, different formulations have been proposed. A recent one has been developed by Curutchet *et al.*¹¹⁹ starting from the density functional scheme originally proposed by Tkatchenko and Scheffler¹²⁰ and generalizing it to a mixed QM-MM description of the atoms. The resulting London-like description of dispersion in terms of effective dipole coefficients is also used to derive a repulsion term by exploiting a Lennard-Jones-like relation. In such a way, both nonelectrostatic contributions are obtained in a single step through the assignment of the dispersion coefficients for the MM sites. By differentiating the dispersion-repulsion energy expression with respect to the QM density, the Fock (or KS) operators are finally obtained. The method, which can treat any atom-type and thus can be applied not only to a solvent but also to more complex environments such as proteins and other biomatrices, has been coupled to an IPD formulation of a polarizable model. A similar approach for dispersion has also been coupled to a polarizable QM/fluctuating charge approach but is applicable only to water as solvent.¹²¹

A different approach for including the Pauli repulsion has been proposed by Olsen *et al.*¹²² still in combination with an IPD approach for polarization effects. Within this model, known as polarizable density embedding (PDE), the system is separated into noncovalently bound fragments, which are divided into a core region, an inner region (the fragments closest to the core), and an outer region. The permanent charge distribution of fragments belonging to the inner region are represented by QM densities, whereas fragments in the outer region are described by atom-centered multipole moments. The combined inner and outer regions comprise an embedding potential. The interactions of the core with the inner region account for a repulsive component in addition to the electrostatic and polarization one. The PDE approach has been recently extended to large biomolecular systems¹²³ using the molecular fractionation with conjugate caps (MFCC)¹²⁴ to partition large molecules into small fragments.

III. PRESENT AND FUTURE APPLICATIONS

As commented before, hybrid QM/classical models have been mostly applied to study solvated molecules (especially in the case of the continuum formulations) and molecules embedded in biological matrices (especially for MM-based formulations). In all cases, the focus has been mainly on the calculation of energies.

In particular, the use of a continuum description where the solvent is characterized by its macroscopic properties, allows a straightforward evaluation of thermodynamic properties, such as solvation free energies. Within this context, the continuum model has to be extended to include nonelectrostatic interactions through the formulations described in Sec. II E. A different and successful strategy to obtain accurate solvation free energies is an extension of COSMO, which is known as COSMO-RS.⁶ Here, the COSMO formulation for electrostatics is supplemented with a statistical thermodynamic treatment to obtain the final solvation free energy.

In the case of QM/MM formulations, a large part of applications has been on the simulation of biological reactivity, especially enzyme-catalyzed reactions. Traditionally, QM/MM studies of enzymatic catalysis have used a potential energy profile or minimum energy pathway

(MEP), which can be obtained by minimizing the energy of the system at several points along the reaction coordinate. In this context, however, multiple enzyme–substrate conformations should be considered as the energy barrier and the transition state structures can significantly vary depending on the starting conformation. To obtain a correct sampling, an extensive MD simulation at fully MM level is commonly used and QM/MM studies of the reaction path are successively applied to selected structures taken from the MD trajectory.^{9,10,125}

Over the years, these traditional applications of QM/continuum and QM/MM approaches have been supplemented with new ones. In particular, there has been a large interest in applying hybrid methods to the modeling of spectroscopies and light–matter interactions. In parallel, the types of environments traditionally modeled by hybrid methods have been extended to include more complex systems. Sections III A and III B attempt to summarize the most recent generalizations and extensions of both QM/continuum and QM/MM approaches (and their coupling) underlying the theoretical advances beyond them.

A. From energies to spectroscopies and dynamics

In Sec. II, we have presented the main methodological aspects of the QM/classical approach starting from the definition of the energy Lagrangian [Eq. (1)] from which the operational equations for the different formulations of the approach are obtained. These equations are the building blocks to extend the QM/classical methods to the calculation of molecular properties and spectroscopies.

In fact, the methodological strategies most commonly used in quantum chemistry to simulate spectroscopies are based on the definition of a given response property as derivative of the (quasi-) energy with respect to some internal (such as nuclear coordinates) and/or external variables (such as electric and magnetic fields).¹²⁶ Within this theoretical framework, analytical derivatives of the energy are needed and their formulation for hybrid models is theoretically easy for both strategies. Furthermore, polarizable models allow one not only to compute the aforementioned response properties but also to account for the screening effect of the environment on the electromagnetic field to which the molecular system responds,^{127–130} allowing for accurate and realistic modeling of various spectroscopies. Nevertheless, there are some relevant specificities between continuum and QM/MM models.

In a continuum solvation model, the macroscopic properties used for describing the solvent are obtained taking into account the sampling of the solvent configurational space; this means that the property of interest can be obtained exactly as in vacuum using a single optimized structure for the molecule. On the contrary, in QM/MM approaches the configurational sampling has to be explicitly accounted for. This is commonly achieved by repeating the calculation of the selected property in many different configurations of the environment with a non-negligible increase in computational cost. Commonly, to obtain a proper sampling of the environment (either a solvent or a biological matrix), molecular dynamics simulations are used, eventually combined with enhanced sampling techniques in those cases where the energy surfaces are characterized by barriers too high to be easily overcome at room temperature.^{131–133} Even when using enhanced explorations, however, the computational cost is generally so large that only fully classical MM-MD trajectories can be effectively used. As a result, the property of interest will be obtained through QM/MM

calculations on MM configurations. This combination of different methods, however, can lead to inaccuracies and in some cases artifacts. In fact, common MM force fields have not been parameterized to give molecular geometries accurate enough to be used for QM calculations. A possible solution to this problem is to precede the QM/MM calculations of the property by a geometry optimization of the QM subsystem in each different MM configuration that is kept frozen. An alternative and more consistent approach is to use the configurations extracted from the MM-MD as a starting point for short QM/MM MD trajectories. Within this framework, a good description of the environment configurational space is combined with an accurate evaluation of the coupling between the nuclear degrees of freedom of the QM subsystem and those of the classical environment. This can be a very appealing approach if one is interested in computing vibrational properties and vibronic effects.

For example, it can be shown that the infrared spectrum is proportional to the Fourier transform of the dipole–dipole autocorrelation function (ACF) that can be extracted directly from a MD simulation as follows:^{134,135}

$$\text{IR}(\omega) \propto \beta \omega^2 \int_0^\infty e^{i\omega t} \langle \boldsymbol{\mu}(t) \boldsymbol{\mu}(0) \rangle dt, \quad (30)$$

where $\beta = 1/k_B T$ is the inverse temperature and ω is the frequency. Similarly, the Raman spectrum is proportional to the Fourier transform of the polarizability ACF. Using this method, instead of the most common one based on normal-mode analysis in harmonic approximation, the anharmonic and finite-temperature effects are also automatically included (even if only approximately from a classical nuclear trajectory). Moreover, the identification of all local minima and the corresponding Hessian is no longer needed, which is an important advantage for large systems with complex potential energy surfaces. The limit of this dynamic approach is the computational cost, which is normally determined by the cost of the QM level as the contribution due to the MM part is generally negligible. However, the situation can change significantly if the MM part is based on polarizable force fields. In that case, in fact, the cost associated with the MM part can be significant and high-performing implementations as those described Sec. IID are required, especially if the approach has to be applied to complex systems such as a solvated protein embedding a chromophore.

Based on the same trajectory, it is also possible to compute vibronic properties, such as absorption lineshapes and resonance Raman scattering, beyond the harmonic approximation, automatically including the effect of the environment. This is achieved by expressing the vibronic coupling in terms of a “spectral density” function (SD), which describes the frequency-dependent linear coupling between the electronic excitation and the nuclear degrees of freedom.^{136–138} The SD can be obtained from the Fourier transform of the ACF of the excitation energy fluctuations, i.e., $C_d(t) = \langle U(t)U(0) \rangle$, where $U(t) = \Delta E(t) - \langle \Delta E \rangle$:

$$J(\omega) = \frac{\beta \omega}{2\pi} \int_{-\infty}^\infty e^{i\omega t} C_d(t) dt. \quad (31)$$

For a molecule embedded in an environment, the peaks of the SD due to internal vibrations are generally accompanied by a low-frequency smooth background due to the motions of the environment. However, the environment also affects the dependence of the excitation energies

of the molecule on the nuclear coordinates and the nuclear trajectory, thus affecting both the equilibrium geometry and the vibrational frequencies. Finally, the absorption spectrum can be computed by convoluting the homogeneous line shape with the inhomogeneous distribution of vertical excitation energies computed along the MD simulations. The accuracy of the calculation is largely determined by the quality of the embedding method used for the excitation energy calculations and of the one used for generating the trajectory. As before, an effective approach would be that of using a fully MM description for generating the MD trajectory and QM/MM calculations of excitation energies along the MM trajectory. This sequential method however presents the same problems about the quality of the MM force fields we have discussed above. As a matter of fact, in this case, the problem can be even worse as the potential energy surface explored by the MM-MD method can be significantly different from that described by the QM/MM method making the calculation of excitation energy fluctuations not reliable for obtaining an accurate SD. To eliminate these problems, it is preferable to use the hybrid QM/MM description for both the MD and the excited state calculations. Once again, the main issue is the computational cost, especially when polarizable FFs are used, which, when excitation energies are needed, should represent a more accurate approach as only a polarizable embedding can properly describe the response of the classical environment to the electronic transition in the QM subsystem. Applications of a fully polarizable QM/MM strategy to the calculations of spectral densities and absorption spectra have been presented for a dye intercalated in DNA^{139,140} and for a keto-carotenoid in the orange carotenoid protein (OCP),¹⁴¹ the complex used in cyanobacteria to regulate the light harvesting (LH) function according to the different light conditions. In particular, in the latter case the polarizable QM/MM strategy has been applied to the simulation and interpretation of the differences observed in the resonance Raman and absorption spectra of the two possible forms of OCP (see Fig. 2). In the inactive (orange) form, OCP contains two different domains that are in contact and they encapsulate the noncovalently bound carotenoid. Upon excitation of the carotenoid, the two domains separate and the carotenoid moves into one domain to become active as a quencher for the LH complexes.¹⁴² The atomistic structure is known for the inactive form of OCP but not for the light-activated one; however, a protein called red carotenoid protein (RCP) has been characterized and shown to represent a faithful model for the carotenoid-embedding domain of the photoactivated form of OCP. In Fig. 2, we report the comparison of the RR and absorption spectra calculated for the inactive orange form of OCP and the RCP model of the active red form.

QM/MM dynamics, however, are not limited only to spectroscopies but have also been applied to chemical and biological (mostly enzymatic) reactions especially when associated with enhanced sampling techniques.^{143–148} Also in these cases, one of the main limitations is the computational cost especially if a polarizable FF is used. However, linear scaling implementations can make these approaches more and more appealing. In particular, they could allow to reduce the QM region to the atoms explicitly involved in the reaction leaving everything else as a polarizable environment without considerable loss in accuracy.

In the context of dynamics, continuum models are not very effective methods as its formulation in a time-dependent framework is neither easy nor unique. Recently, real-time (RT) time-dependent density

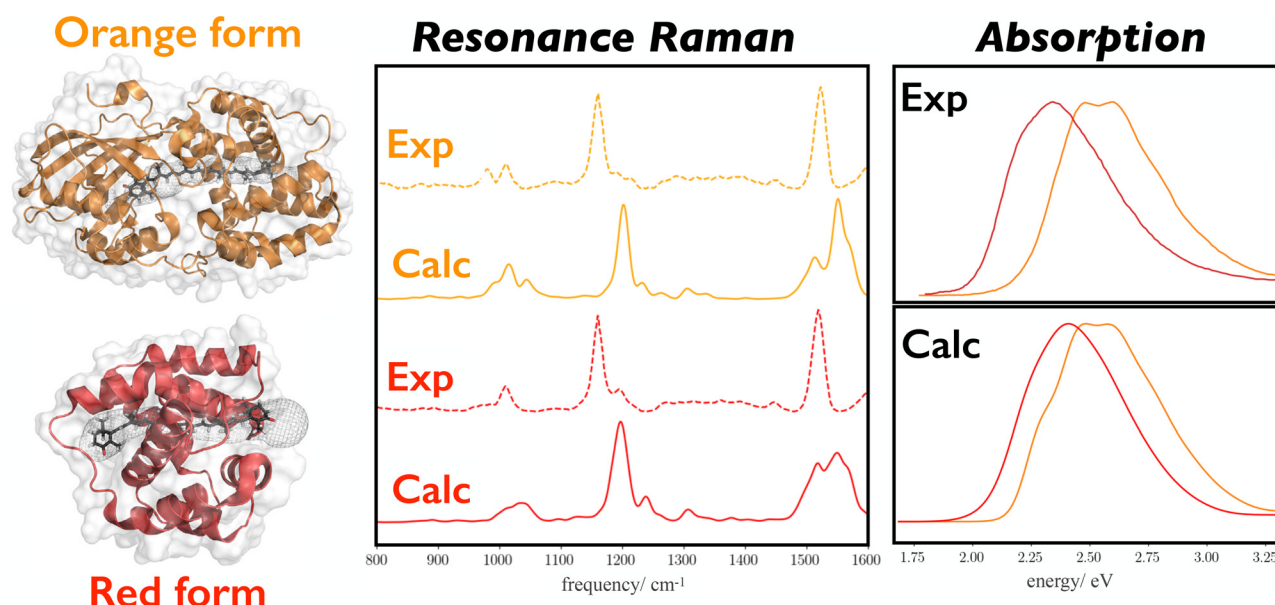


FIG. 2. Comparison of experimental and calculated (left) resonance Raman and (right) absorption spectra of the orange and red forms of OCP. The calculated spectra were obtained combining a polarizable QM/MM BO-MD simulation at the B3LYP/6-31G(d) level with excited state energies computed using the same polarizable hybrid approach where the QM level was TD-CAM-B3LYP/6-31+G(d). In all cases, the polarizable embedding (protein, water molecules, and ions) was described through the AMEBA force field. Adapted from Bondanza *et al.*, "The multiple roles of the protein in the photoactivation of orange carotenoid protein," *Chem* **6**, 187–203 (2020). Copyright 2020 Cell Press.

functional formulations have been proposed for PCM models^{149,150} using the full spectrum of the frequency-dependent dielectric permittivity of the solvent. The resulting time-dependent ASCs are used in combination with the quantum equation describing the time evolution of the electronic degrees of freedom of the solute. As a result, the QM density propagates in the presence of an environment that accounts for the delayed solvent response (nonequilibrium effects). These approaches are mostly focused on the description of the time evolution of electronic density following a perturbation and as such they are generally used for simulating spectroscopy. On the contrary, their extension to include nuclear dynamics is neither straightforward nor computationally effective.

The extension of hybrid QM/classical methods to dynamics is not limited to ground state systems. In particular, QM/MM approaches have been largely used in photochemical studies of solvated molecules and chromophores embedded in biological matrices (DNA or proteins).^{13,151} In its most straightforward formulation, QM/MM dynamics uses a classical approximation for the nuclear motion in combination with a Born–Oppenheimer (BO) picture, so that the evolution is fully determined by the potential energy surface of the associated adiabatic electronic state. In many light-driven processes, however, the BO approximation breaks down and a nonadiabatic dynamics has to be modeled. Also in this case, however, a common strategy is that of conserving a classical approximation for the nuclear motion, obtaining the so-called mixed quantum-classical nonadiabatic schemes.^{14,152–154} Among them, the most commonly used is the trajectory-based surface hopping (SH), pioneered by Tully.^{155,156} SH simulations are easily extended to QM/MM methods based on an electrostatic embedding. Within this framework, in fact, the atoms of the

environment are described by fixed point charges behaving classically. As a result, their presence only increases the number of coordinates to be treated in the classical equation of motion. Moreover, the additional electrostatic contribution to the forces acting on the QM subsystem can be obtained exactly in the same way one calculates the effects of the nuclei. As a result, SH QM/MM simulations can be performed with only a limited increase in the computational cost. On the contrary, the use of a polarizable QM/MM formulation introduces some specificities that need to be carefully considered.^{157,158} The main point is that each electronic state of the QM system polarizes the classical part in a different way and is then characterized by a different Hamiltonian. This results in a difficulty in the vicinity of avoided crossings and conical intersections, which is not present for nonpolarizable MM descriptions. Approximated solutions are possible but, so far, no SH (or more in general, trajectory-based) nonadiabatic simulations with polarizable MM FF have been reported in the literature.

B. From solvents and biomatrices to composite systems

Hybrid QM/classical methods are by definition multiscale approaches; as such, they are ideal candidates to model composite systems where different “objects” of molecular, nano-, and mesoscopic scales are coupled together. An important example of how hybrid QM/classical approaches can be effectively used in studying composite systems is represented by heterogeneous catalysis.¹⁵⁹ Nowadays, heterogeneous catalysis is usually performed using catalysts composed of metallic nanoparticles deposited on an oxide support and surrounded by a solvent. If the catalyst particles are significantly larger than the molecular scale, periodic slab models are generally used. However,

these models become too costly when applied to systems of low symmetry such as surfaces with defects. In these cases, QM/MM models are an effective alternative, as only a small portion of the system (the defect, for example) is treated at a QM level, whereas the rest is treated classically. When the catalyst particles are subnanometer clusters, slab models are no more applicable and discrete cluster models have to be used. In these cases, however, a further complexity is represented by the catalyst support affecting the catalytic activity of clusters. Because of that, an explicit atomistic model for the catalyst-support interactions is often needed. On top of that, a third component can play an important role and has to be included in the model: the solvent. In the field of heterogeneous catalytic reactions, and especially in electrocatalytic systems, a popular approach to include solvent effects is through those formulations of continuum models that use a smooth transition at the solute-solvent interface.^{32,160} Continuum models, however, cannot describe specific and directional interactions between the solute and solvent. An obvious way to go would be to introduce an atomistic MM model for the solvent combined with MD simulations for sampling the configurational space of the solvated system. This strategy, however, generally implies a large computational cost and hybrid-cluster-continuum models are generally used.¹⁶¹ Within this framework, specific and directional interactions are treated through a set of explicit solvent molecules and long-range electrostatic interactions by using continuum models.

Another interesting application of QM/classical approaches to composite systems is aimed at modeling the effects of light radiation on a solvated molecule in the proximity of a metallic nanoparticle (MNP).^{15,17,162} Under proper conditions, light can excite a collective excitation of the metal conduction electrons (a plasmon) and great amplifications of the electric field at the molecular site can be achieved. This amplification is exactly what is exploited in surface-enhanced (SE) spectroscopies,¹⁶³ among which SE Raman spectroscopy (SERS; or metallic tip-enhanced Raman spectroscopy, TERS)^{164,165} is the most well-known example. Moreover, plasmonic NPs are also used to promote photochemical reactions.¹⁶⁶ The reason why QM/classical models represent an effective strategy to investigate nanoplasmonics is not only that an accurate QM representation of the MNP is unfeasible for systems larger than a few nanometers. The MNP, in fact, can be seen as an effective environment that can feel and react to the molecular probe and the external electromagnetic field. Therefore, a classical model that includes both these responses is generally enough to study plasmon-enhanced spectroscopies and plasmon-modified chemical reactions. Also here, the QM/classical approaches for nanoplasmonics can either use a continuum description or introduce a classical but atomistic model for the NP.

In the continuum formulations, the NP is treated as a dielectric particle of given size and shape, and a frequency-dependent permittivity function $\epsilon(\omega)$ is introduced to describe the NP electromagnetic response to the external field. In the QM/MM formulation, different formulations have been proposed so far. The most common one uses both atomic polarizabilities and capacitances.^{167,168}

The continuum formulation of metal nanoparticles has been also extended to include a polarizable MM region. This is an example of the three-layer model we have discussed in Sec. II: also here the model is fully self-consistent and it accounts for the mutual polarizations of the QM, the MM, and the continuum MNP(s). The model has been mostly used to investigate how the MNP (a sphere, a rod, or a tip)

affects the excitonic states of LH pigment-protein complexes. Experimental studies have in fact demonstrated the ability of metal NPs to drastically manipulate the optical properties of single LH complexes.^{169–172} The model is built by combining a polarizable QM/MM excitonic approach^{173,174} to describe the LH complex with a continuum description of the MNP and the solvent. When applied to the study of the LH complex peridinin-chlorophyll-protein (PCP) in the presence of silver nanoparticles, it correctly reproduced the experimental amplification of the PCP fluorescence signal (see Fig. 3).¹⁷⁵ Successively, the same model was used to investigate how a plasmonic nanostructure affects excitonic states of the main LH complex (LH2) of purple bacteria.^{176,177} Once again, the simulations not only reproduce the observed enhancement of fluorescence of LH2 when coupled to a gold nanorod but also suggest that by modifying the nanorod into a nanotip, a drastic perturbation of the exciton states can be achieved, inducing localization effects of varying degrees.

IV. OUTLOOK

Hybrid QM/classical methods, in their continuum, atomistic, or multilayer formulations, represent a mature and potent strategy to simulate energies, structures, properties, and processes of systems of increasing complexity. The modularity in the QM and classical layers and the possibility to couple them with a hierarchy of approximations of increasing completeness and accuracy make these multiscale methods extremely flexible and easy to adapt to very different problems in chemistry, biology, materials science, and beyond.

Thanks to these unique characteristics, hybrid methods will continue to play a fundamental role in the years to come. However, the

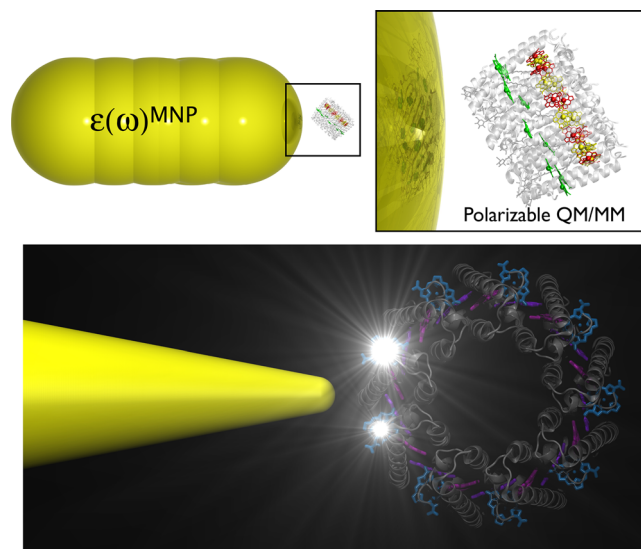


FIG. 3. Top: schematic representation of the nanorod-LH2 assembly used to simulate the experiments. Bottom: pictorial representation of the setup suggested by simulations to induce localizations in the exciton states of the LH2 complex. Adapted from S. Caprasecca, C. A. Guido, and B. Mennucci, "Control of coherences and optical responses of pigment-protein complexes by plasmonic nanoantennae." *J. Phys. Chem. Lett.* **7**, 2189–2196 (2016). Copyright 2016 American Chemical Society. Adapted from S. Caprasecca, S. Corni, and B. Mennucci, "Shaping excitons in light-harvesting proteins through nanoplasmonics." *Chem. Sci.* **9**, 6219–6227 (2018). Copyright 2018 Royal Society of Chemistry.

impact that they will have will be largely determined by three elements.

The first one is the quality of their computational implementation. In other words, the traditional assumption that the cost associated with the embedding model is negligible with respect to the cost of the QM method needs to be rethought, and an important effort in the crafting of fast algorithms and optimized implementations has to become a priority. The use of multiscale models to describe large, complex systems requires, in fact, the availability of linear scaling implementations. The deployment of such implementations on modern hardware, including parallel computers and graphic processor units, is also paramount.

Second, the change in the way hybrid methods have to be formulated and implemented has to be accompanied by a more standardized and reproducible way in which they are applied. As for the QM description where the level of theory is fully defined only when all the connected features (basis set, DFT functional, active space, etc.) are defined, the same should apply for the hybrid methods. For example, for continuum models, the specific formulation used should be indicated, together with the parameters that define the molecular cavity and discretization: only in this way, in fact, calculations can be reproducible. In parallel, QM/MM applications should report all the information related to the MM force field; the type of embedding (with indication of the model used to treat bonds between QM and MM atoms, if any); and the presence of eventual cutoff in the QM-MM and MM-MM interactions. The effectiveness of this important standardization clearly goes through a common effort by the software developing community, which needs to make the different implementations not only available to the scientific community (possibly open source) but also well-documented and tested in all their parts.

Finally, hybrid methods will be even more successful in facing future challenges of the modeling of complex systems if they will be able to integrate the many potentialities of machine learning (ML) techniques. In particular, ML techniques could allow us to define new and more accurate FFs, enable a proper sampling for very large and complex systems, and extend (nonadiabatic) dynamics simulation in space and time.^{178–180} As a matter of fact, hybrid ML/MM/(continuum) methods are promising methods to further extend the boundaries of QM-based descriptions to large and complex systems.^{181,182}

ACKNOWLEDGMENTS

The authors acknowledge funding by the European Research Council, under Grant No. ERC-AdG-786714 (LIFETimeS).

DATA AVAILABILITY

The data that support the findings of this study are available from the corresponding authors upon reasonable request.

REFERENCES

- ¹A. Warshel and M. Levitt, "Theoretical studies of enzymic reactions: Dielectric, electrostatic and steric stabilization of the carbonium ion in the reaction of lysozyme," *J. Mol. Biol.* **103**, 227–249 (1976).
- ²J. L. Rivail and D. Rinaldi, "A quantum chemical approach to dielectric solvent effects in molecular liquids," *Chem. Phys.* **18**, 233–242 (1976).
- ³S. Miertuš, E. Scrocco, and J. Tomasi, "Electrostatic interaction of a solute with a continuum. A direct utilization of AB initio molecular potentials for the prevision of solvent effects," *Chem. Phys.* **55**, 117–129 (1981).
- ⁴C. J. Cramer and D. G. Truhlar, "Implicit solvation models: Equilibria, structure, spectra, and dynamics," *Chem. Rev.* **99**, 2161–2200 (1999).
- ⁵J. Tomasi, B. Mennucci, and R. Cammi, "Quantum mechanical continuum solvation models," *Chem. Rev.* **105**, 2999–3093 (2005).
- ⁶A. Klamt, "The COSMO and COSMO-RS solvation models," *WIREs Comput. Mol. Sci.* **1**, 699–709 (2011).
- ⁷H. M. Senn and W. Thiel, "QM/MM studies of enzymes," *Curr. Opin. Chem. Biol.* **11**, 182–187 (2007).
- ⁸M. W. van der Kamp and A. J. Mulholland, "Combined quantum mechanics/molecular mechanics (QM/MM) methods in computational enzymology," *Biochemistry* **52**, 2708–2728 (2013).
- ⁹K. Świderek, I. Tuñón, and V. Moliner, "Predicting enzymatic reactivity: From theory to design," *Wiley Interdiscip. Rev.: Comput. Mol. Sci.* **4**, 407–421 (2013).
- ¹⁰S. F. Sousa, A. J. M. Ribeiro, R. P. P. Neves, N. F. Brás, N. M. F. S. A. Cerqueira, P. A. Fernandes, and M. J. Ramos, "Application of quantum mechanics/molecular mechanics methods in the study of enzymatic reaction mechanisms," *Wiley Interdiscip. Rev.: Comput. Mol. Sci.* **7**, e1281 (2017).
- ¹¹B. Mennucci, "Modeling environment effects on spectroscopies through QM/classical models," *Phys. Chem. Chem. Phys.* **15**, 6583–6594 (2013).
- ¹²U. N. Morzan, D. J. Alonso de Armiño, N. O. Foglia, F. Ramírez, M. C. González Lebrero, D. A. Scherlis, and D. A. Estrin, "Spectroscopy in complex environments from QM-MM simulations," *Chem. Rev.* **118**, 4071–4113 (2018).
- ¹³E. Brunk and U. Rothlisberger, "Mixed quantum mechanical/molecular mechanical molecular dynamics simulations of biological systems in ground and electronically excited states," *Chem. Rev.* **115**, 6217–6263 (2015).
- ¹⁴T. R. Nelson, A. J. White, J. A. Bjorgaard, A. E. Sifain, Y. Zhang, B. Nebgen, S. Fernandez-Alberti, D. Mozysky, A. E. Roitberg, and S. Tretiak, "Non-adiabatic excited-state molecular dynamics: Theory and applications for modeling photophysics in extended molecular materials," *Chem. Rev.* **120**, 2215–2287 (2020).
- ¹⁵B. Mennucci and S. Corni, "Multiscale modelling of photoinduced processes in composite systems," *Nat. Rev. Chem.* **3**, 315–330 (2019).
- ¹⁶F. Segatta, L. Cupellini, M. Garavelli, and B. Mennucci, "Quantum chemical modeling of the photoinduced activity of multichromophoric biosystems," *Chem. Rev.* **119**, 9361–9380 (2019).
- ¹⁷E. Coccia, J. Fregoni, C. A. Guido, M. Marsili, S. Pipolo, and S. Corni, "Hybrid theoretical models for molecular nanoplasmonics," *J. Chem. Phys.* **153**, 200901 (2020).
- ¹⁸M. Nottoli and F. Lipparini, "General formulation of polarizable embedding models and of their coupling," *J. Chem. Phys.* **153**, 224108 (2020).
- ¹⁹F. del Valle and J. Tomasi, "Electron correlation and solvation effects. I. Basic formulation and preliminary attempt to include the electron correlation in the quantum mechanical polarizable continuum model so as to study solvation phenomena," *Chem. Phys.* **150**, 139–150 (1991).
- ²⁰J. G. Ángyán, "Choosing between alternative mp2 algorithms in the self-consistent reaction field theory of solvent effects," *Chem. Phys. Lett.* **241**, 51–56 (1995).
- ²¹F. Lipparini, G. Scalmani, and B. Mennucci, "Non covalent interactions in RNA and DNA base pairs: A quantum-mechanical study of the coupling between solvent and electronic density," *Phys. Chem. Chem. Phys.* **11**, 11617–11623 (2009).
- ²²O. Christiansen and K. V. Mikkelsen, "A coupled-cluster solvent reaction field method," *J. Chem. Phys.* **110**, 1365–1375 (1999).
- ²³O. Christiansen and K. V. Mikkelsen, "Coupled cluster response theory for solvated molecules in equilibrium and nonequilibrium solvation," *J. Chem. Phys.* **110**, 8348–8360 (1999).
- ²⁴R. Cammi, R. Fukuda, M. Ehara, and H. Nakatsuji, "Symmetry-adapted cluster and symmetry-adapted cluster-configuration interaction method in the polarizable continuum model: Theory of the solvent effect on the electronic excitation of molecules in solution," *J. Chem. Phys.* **133**, 024104–024125 (2010).
- ²⁵R. Cammi, "Quantum cluster theory for the polarizable continuum model. I. The CCSD level with analytical first and second derivatives," *J. Chem. Phys.* **131**, 164104 (2009).

- ²⁶M. Caricato, B. Mennucci, G. Scalmani, G. W. Trucks, and M. J. Frisch, "Electronic excitation energies in solution at equation of motion CCSD level within a state specific polarizable continuum model approach," *J. Chem. Phys.* **132**, 084102 (2010).
- ²⁷M. Caricato, G. Scalmani, G. W. Trucks, and M. J. Frisch, "Coupled cluster calculations in solution with the polarizable continuum model of solvation," *J. Phys. Chem. Lett.* **1**, 2369–2373 (2010).
- ²⁸M. Caricato, "Ccsd-pcm: Improving upon the reference reaction field approximation at no cost," *J. Chem. Phys.* **135**, 074113 (2011).
- ²⁹B. Lunkenheimer and A. Köhn, "Solvent effects on electronically excited states using the conductor-like screening model and the second-order correlated method ADC(2)," *J. Chem. Theory Comput.* **9**, 977–994 (2013).
- ³⁰M. Caricato, F. Lipparini, G. Scalmani, C. Cappelli, and V. Barone, "Vertical electronic excitations in solution with the EOM-CCSD method combined with a polarizable explicit/implicit solvent model," *J. Chem. Theory Comput.* **9**, 3035–3042 (2013).
- ³¹S. Ren, F. Lipparini, B. Mennucci, and M. Caricato, "Coupled cluster theory with induced dipole polarizable embedding for ground and excited states," *J. Chem. Theory Comput.* **15**, 4485–4496 (2019).
- ³²O. Andreussi, I. Dabo, and N. Marzari, "Revised self-consistent continuum solvation in electronic-structure calculations," *J. Chem. Phys.* **136**, 064102 (2012).
- ³³S. Zhou, L.-T. Cheng, J. Dzubiella, B. Li, and J. A. McCammon, "Variational implicit solvation with Poisson–Boltzmann theory," *J. Chem. Theory Comput.* **10**, 1454–1467 (2014).
- ³⁴S. Ringe, H. Oberhofer, C. Hille, S. Matera, and K. Reuter, "Function-space-based solution scheme for the size-modified Poisson–Boltzmann equation in full-potential DFT," *J. Chem. Theory Comput.* **12**, 4052–4066 (2016).
- ³⁵S. Ringe, H. Oberhofer, and K. Reuter, "Transferable ionic parameters for first-principles Poisson–Boltzmann solvation calculations: Neutral solutes in aqueous monovalent salt solutions," *J. Chem. Phys.* **146**, 134103 (2017).
- ³⁶G. Fisicaro, L. Genovese, O. Andreussi, S. Mandal, N. N. Nair, N. Marzari, and S. Goedecker, "Soft-sphere continuum solvation in electronic-structure calculations," *J. Chem. Theory Comput.* **13**, 3829–3845 (2017).
- ³⁷J. C. Womack, L. Anton, J. Dziedzic, P. J. Hasnip, M. I. J. Probert, and C.-K. Skylaris, "DL_mg: A parallel multigrid Poisson and Poisson–Boltzmann solver for electronic structure calculations in vacuum and solution," *J. Chem. Theory Comput.* **14**, 1412–1432 (2018).
- ³⁸M. P. Coons and J. M. Herbert, "Quantum chemistry in arbitrary dielectric environments: Theory and implementation of nonequilibrium Poisson boundary conditions and application to compute vertical ionization energies at the air/water interface," *J. Chem. Phys.* **148**, 222834 (2018).
- ³⁹B. Mennucci, "Polarizable continuum model," *WIREs Comput. Mol. Sci.* **2**, 386–404 (2012).
- ⁴⁰A. Klamt and G. Schuurmann, "Cosmo: A new approach to dielectric screening in solvents with explicit expressions for the screening energy and its gradient," *J. Chem. Soc. Perkin Trans. 2*, 799–805 (1993).
- ⁴¹V. Barone and M. Cossi, "Quantum calculation of molecular energies and energy gradients in solution by a conductor solvent model," *J. Phys. Chem. A* **102**, 1995–2001 (1998).
- ⁴²D. Chipman, "Simulation of volume polarization in reaction field theory," *J. Chem. Phys.* **110**, 8012–8018 (1999).
- ⁴³B. Mennucci, E. Cancès, and J. Tomasi, "Evaluation of solvent effects in isotropic and anisotropic dielectrics and in ionic solutions with a unified integral equation method: Theoretical bases, computational implementation, and numerical applications," *J. Phys. Chem. B* **101**, 10506–10517 (1997).
- ⁴⁴E. Cancès, "Integral equation approaches for continuum models," in *Continuum Solvation Models in Chemical Physics*, edited by B. Mennucci and R. Cammi (Wiley, New York, 2007), Chap. 1.2, pp. 29–48.
- ⁴⁵R. Cammi and J. Tomasi, "Remarks on the use of the apparent surface-charges (ASC) methods in solvation problems—Iterative versus matrix-inversion procedures and the renormalization of the apparent charges," *J. Comput. Chem.* **16**, 1449–1458 (1995).
- ⁴⁶D. York and M. Karplus, "A smooth solvation potential based on the conductor-like screening model," *J. Phys. Chem. A* **103**, 11060–11079 (1999).
- ⁴⁷G. Scalmani and M. J. Frisch, "Continuous surface charge polarizable continuum models of solvation. I. General formalism," *J. Chem. Phys.* **132**, 114110 (2010).
- ⁴⁸A. W. Lange and J. M. Herbert, "Polarizable continuum reaction-field solvation models affording smooth potential energy surfaces," *J. Phys. Chem. Lett.* **1**, 556–561 (2010).
- ⁴⁹A. W. Lange and J. M. Herbert, "A smooth, nonsingular, and faithful discretization scheme for polarizable continuum models: The switching/Gaussian approach," *J. Chem. Phys.* **133**, 244111 (2010).
- ⁵⁰A. W. Lange and J. M. Herbert, "Symmetric versus asymmetric discretization of the integral equations in polarizable continuum solvation models," *Chem. Phys. Lett.* **509**, 77–87 (2011).
- ⁵¹F. Lipparini, G. Scalmani, B. Mennucci, E. Cancès, M. Caricato, and M. J. Frisch, "A variational formulation of the polarizable continuum model," *J. Chem. Phys.* **133**, 014106 (2010).
- ⁵²J.-L. Fattebert and F. Gygi, "Density functional theory for efficient *ab initio* molecular dynamics simulations in solution," *J. Comput. Chem.* **23**, 662–666 (2002).
- ⁵³D. Bashford and D. A. Case, "Generalized born models of macromolecular solvation effects," *Ann. Rev. Phys. Chem.* **51**, 129–152 (2000).
- ⁵⁴S. Cardamone, T. J. Hughes, and P. L. A. Popelier "Multipolar electrostatics," *Phys. Chem. Chem. Phys.* **16**, 10367–10387 (2014).
- ⁵⁵J. M. H. Olsen, N. H. List, K. Kristensen, and J. Kongsted, "Accuracy of protein embedding potentials: An analysis in terms of electrostatic potentials," *J. Chem. Theory Comput.* **11**, 1832–1842 (2015).
- ⁵⁶M. T. P. Beerepoot, A. H. Steindal, N. H. List, J. Kongsted, and J. M. H. Olsen, "Averaged solvent embedding potential parameters for multiscale modeling of molecular properties," *J. Chem. Theory Comput.* **12**, 1684–1695 (2016).
- ⁵⁷M. S. Nørby, C. Steinmann, J. M. H. Olsen, H. Li, and J. Kongsted, "Computational approach for studying optical properties of DNA systems in solution," *J. Chem. Theory Comput.* **12**, 5050–5057 (2016).
- ⁵⁸T. A. Halgren and W. Damm, "Polarizable force fields," *Curr. Opin. Struct. Biol.* **11**, 236–242 (2001).
- ⁵⁹A. Warshel, M. Kato, and A. V. Pislakov, "Polarizable force fields: History, test cases, and prospects," *J. Chem. Theory Comput.* **3**, 2034–2045 (2007).
- ⁶⁰P. Cieplak, F.-Y. Dupradeau, Y. Duan, and J. Wang, "Polarization effects in molecular mechanical force fields," *J. Phys.: Condens. Matter* **21**, 333102–333122 (2009).
- ⁶¹Z. Jing, C. Liu, S. Y. Cheng, R. Qi, B. D. Walker, J.-P. Piquemal, and P. Ren, "Polarizable force fields for biomolecular simulations: Recent advances and applications," *Annu. Rev. Biophys.* **48**, 371–394 (2019).
- ⁶²A. Rappe and W. Goddard, "Charge equilibration for molecular-dynamics simulations," *J. Phys. Chem.* **95**, 3358–3363 (1991).
- ⁶³S. W. Rick, S. J. Stuart, and B. J. Berne, "Dynamical fluctuating charge force fields: Application to liquid water," *J. Chem. Phys.* **101**, 6141–6156 (1994).
- ⁶⁴P. P. Poier and F. Jensen, "Describing molecular polarizability by a bond capacity model," *J. Chem. Theory Comput.* **15**, 3093–3107 (2019).
- ⁶⁵F. Lipparini, C. Cappelli, and V. Barone, "A gauge invariant multiscale approach to magnetic spectroscopies in condensed phase: General three-layer model, computational implementation and pilot applications," *J. Chem. Phys.* **138**, 234108 (2013).
- ⁶⁶C. Cappelli, "Integrated QM/polarizable mm/continuum approaches to model chiroptical properties of strongly interacting solute–solvent systems," *Int. J. Quantum Chem.* **116**, 1532–1542 (2016).
- ⁶⁷A. Warshel, M. Kato, and A. V. Pislakov, "Polarizable force fields: History, test cases, and prospects," *J. Chem. Theory Comput.* **3**, 2034–2045 (2007).
- ⁶⁸M. A. Thompson and G. K. Schenter, "Excited states of the bacteriochlorophyll b dimer of Rhodospseudomonas viridis: A QM/MM study of the photo-synthetic reaction center that includes MM polarization," *J. Phys. Chem.* **99**, 6374–6386 (1995).
- ⁶⁹J. Gao, "Energy components of aqueous solution: Insight from hybrid QM/MM simulations using a polarizable solvent model," *J. Comput. Chem.* **18**, 1061–1071 (1997).
- ⁷⁰P. T. van Duijnen and M. Swart, "Molecular and atomic polarizabilities: Thole's model revisited," *J. Phys. Chem. A* **102**, 2399 (1998).
- ⁷¹D. Loco, É. Polack, S. Caprasecca, L. Lagardère, F. Lipparini, J.-P. Piquemal, and B. Mennucci, "A QM/MM approach using the amoeba polarizable embedding: From ground state energies to electronic excitations," *J. Chem. Theory Comput.* **12**, 3654–3661 (2016).

- ⁷²J. M. H. Olsen and J. Kongsted, *Chapter 3 - Molecular Properties through Polarizable Embedding* (Academic Press, 2011), pp. 107–143.
- ⁷³Y. Mao, Y. Shao, J. Dziedzic, C.-K. Skylaris, T. Head-Gordon, and M. Head-Gordon, “Performance of the amoeba water model in the vicinity of QM solutes: A diagnosis using energy decomposition analysis,” *J. Chem. Theory Comput.* **13**, 1963–1979 (2017).
- ⁷⁴J. Dziedzic, Y. Mao, Y. Shao, J. Ponder, T. Head-Gordon, M. Head-Gordon, and C.-K. Skylaris, “Tinkert: A fully self-consistent, mutually polarizable QM/MM approach based on the amoeba force field,” *J. Chem. Phys.* **145**, 124106 (2016).
- ⁷⁵X. Wu, J.-M. Teuler, F. Cailliez, C. Clavaguéra, D. R. Salahub, and A. de la Lande, “Simulating electron dynamics in polarizable environments,” *J. Chem. Theory Comput.* **13**, 3985–4002 (2017).
- ⁷⁶J. W. Ponder, C. Wu, P. Ren, V. S. Pande, J. D. Chodera, M. J. Schnieders, I. Haque, D. L. Mobley, D. S. Lambrecht, R. A. DiStasio, Jr., M. Head-Gordon, G. N. I. Clark, M. E. Johnson, and T. Head-Gordon, “Current status of the AMOEBA polarizable force field,” *J. Phys. Chem. B* **114**, 2549–2564 (2010).
- ⁷⁷D. Loco, L. Lagardère, S. Caprasecca, F. Lipparini, B. Mennucci, and J.-P. Piquemal, “Hybrid QM/MM molecular dynamics with amoeba polarizable embedding,” *J. Chem. Theory Comput.* **13**, 4025–4033 (2017).
- ⁷⁸M. Nottoli, B. Mennucci, and F. Lipparini, “Excited state Born-Oppenheimer molecular dynamics through a coupling between time dependent DFT and AMOEBA,” *Phys. Chem. Chem. Phys.* **22**, 19532–19541 (2020).
- ⁷⁹E. Boulanger and W. Thiel, “Solvent boundary potentials for hybrid QM/MM computations using classical Drude oscillators: A fully polarizable model,” *J. Chem. Theory Comput.* **8**, 4527–4538 (2012).
- ⁸⁰S. Riahi and C. N. Rowley, “The Charmm–Turbomole interface for efficient and accurate QM/MM molecular dynamics, free energies, and excited state properties,” *J. Comput. Chem.* **35**, 2076–2086 (2014).
- ⁸¹C. N. Rowley and B. Roux, “The solvation structure of Na⁺ and K⁺ in liquid water determined from high level *ab initio* molecular dynamics simulations,” *J. Chem. Theory Comput.* **8**, 3526–3535 (2012).
- ⁸²S. K. Sahoo and N. N. Nair, “Interfacing the core-shell or the Drude polarizable force field with Car–Parrinello molecular dynamics for QM/MM simulations,” *Front. Chem.* **6**, 275 (2018).
- ⁸³Z. Lu and Y. Zhang, “Interfacing *ab initio* quantum mechanical method with classical Drude oscillator model for molecular dynamics simulation of chemical reactions,” *J. Chem. Theory Comput.* **4**, 1237–1248 (2008).
- ⁸⁴J. A. Lemkul, J. Huang, B. Roux, and A. D. MacKerell, Jr., “An empirical polarizable force field based on the classical Drude oscillator model: Development history and recent applications,” *Chem. Rev.* **116**, 4983–5013 (2016).
- ⁸⁵M. S. Gordon, D. G. Fedorov, S. R. Pruitt, and L. V. Slipchenko, “Fragmentation methods: A route to accurate calculations on large systems,” *Chem. Rev.* **112**, 632–672 (2012).
- ⁸⁶T. A. Wesolowski and A. Warshel, “Frozen density functional approach for *ab initio* calculations of solvated molecules,” *J. Phys. Chem.* **97**, 8050–8053 (1993).
- ⁸⁷T. A. Wesolowski, S. Shedge, and X. Zhou, “Frozen-density embedding strategy for multilevel simulations of electronic structure,” *Chem. Rev.* **115**, 5891–5928 (2015).
- ⁸⁸C. R. Jacob and J. Neugebauer, “Subsystem density-functional theory,” *WIREs Comput. Mol. Sci.* **4**, 325–362 (2014).
- ⁸⁹M. S. Gordon, M. A. Freitag, P. Bandyopadhyay, J. H. Jensen, V. Kairys, and W. J. Stevens, “The effective fragment potential method: A QM-based mm approach to modeling environmental effects in chemistry,” *J. Phys. Chem. A* **105**, 293–307 (2001).
- ⁹⁰M. S. Gordon, Q. A. Smith, P. Xu, and L. V. Slipchenko, “Accurate first principles model potentials for intermolecular interactions,” *Ann. Rev. Phys. Chem.* **64**, 553–578 (2013).
- ⁹¹J. Gao, D. G. Truhlar, Y. Wang, M. J. M. Mazack, P. Löffler, M. R. Provorse, and P. Rehak, “Explicit polarization: A quantum mechanical framework for developing next generation force fields,” *Acc. Chem. Res.* **47**, 2837–2845 (2014).
- ⁹²H. M. Senn and W. Thiel, “Qm/mm methods for biological systems,” in *Atomistic Approaches in Modern Biology: From Quantum Chemistry to Molecular Simulations*, edited by M. Reiher (Springer Berlin Heidelberg, Berlin, Heidelberg, 2007), pp. 173–290.
- ⁹³A. Monari, J.-L. Rivail, and X. Assfeld, “Theoretical modeling of large molecular systems. Advances in the local self consistent field method for mixed quantum mechanics/molecular mechanics calculations,” *Acc. Chem. Res.* **46**, 596–603 (2013).
- ⁹⁴T. Vreven, B. Mennucci, C. da Silva, K. Morokuma, and J. Tomasi, “The ONIOM-PCM method: Combining the hybrid molecular orbital method and the polarizable continuum model for solvation. Application to the geometry and properties of a merocyanine in solution,” *J. Chem. Phys.* **115**, 62–72 (2001).
- ⁹⁵F. Lipparini, C. Cappelli, G. Scalmani, N. De Mitri, and V. Barone, “Analytical first and second derivatives for a fully polarizable QM/classical Hamiltonian,” *J. Chem. Theory Comput.* **8**, 4270–4278 (2012).
- ⁹⁶T. Giovannini, A. Puglisi, M. Ambrosetti, and C. Cappelli, “Polarizable QM/MM approach with fluctuating charges and fluctuating dipoles: The QM/FQFμ model,” *J. Chem. Theory Comput.* **15**, 2233–2245 (2019).
- ⁹⁷T. Benighaus and W. Thiel, “A general boundary potential for hybrid QM/MM simulations of solvated biomolecular systems,” *J. Chem. Theory Comput.* **5**, 3114–3128 (2009).
- ⁹⁸T. Benighaus and W. Thiel, “Efficiency and accuracy of the generalized solvent boundary potential for hybrid QM/MM simulations: Implementation for semiempirical hamiltonians,” *J. Chem. Theory Comput.* **4**, 1600–1609 (2008).
- ⁹⁹A. H. Steindl, K. Ruud, L. Frediani, K. Aidas, and J. Kongsted, “Excitation energies in solution: The fully polarizable QM/MM/PCM method,” *J. Phys. Chem. B* **115**, 3027–3037 (2011).
- ¹⁰⁰S. Caprasecca, C. Curutchet, and B. Mennucci, “Toward a unified modeling of environment and bridge-mediated contributions to electronic energy transfer: A fully polarizable QM/MM/PCM approach,” *J. Chem. Theory Comput.* **8**, 4462–4473 (2012).
- ¹⁰¹S. Caprasecca, S. Jurinovich, L. Lagardère, B. Stamm, and F. Lipparini, “Achieving linear scaling in computational cost for a fully polarizable mm/continuum embedding,” *J. Chem. Theory Comput.* **11**, 694–704 (2015).
- ¹⁰²M. Corbella, L. Cupellini, F. Lipparini, G. D. Scholes, and C. Curutchet, “Spectral variability in phycocyanin cryptophyte antenna complexes is controlled by changes in the α -polypeptide chains,” *ChemPhotoChem* **3**, 945–956 (2019).
- ¹⁰³L. Greengard and V. Rokhlin, “A fast algorithm for particle simulations,” *J. Comput. Phys.* **73**, 325–348 (1987).
- ¹⁰⁴G. Scalmani, V. Barone, K. Kudin, C. Pomelli, G. Scuseria, and M. Frisch, “Achieving linear-scaling computational cost for the polarizable continuum model of solvation,” *Theor. Chem. Acc.* **111**, 90–100 (2004).
- ¹⁰⁵J. M. Herbert and A. W. Lange, “Polarizable continuum models for (bio)molecular electrostatics: Basic theory and recent developments for macromolecules and simulations,” in *Many-Body Effects and Electrostatics in Biomolecules*, edited by Q. Cui, P. Ren, and M. Meuwly (Pan, Stanford, 2016), Chap. 11, pp. 363–416.
- ¹⁰⁶F. Lipparini, “General linear scaling implementation of polarizable embedding schemes,” *J. Chem. Theory Comput.* **15**, 4312–4317 (2019).
- ¹⁰⁷M. Scheurer, P. Reinholdt, J. M. H. Olsen, A. Dreuw, and J. Kongsted, “Efficient open-source implementations of linear-scaling polarizable embedding: Use ootrees to save the trees,” *J. Chem. Theory Comput.* **17**, 3445–3454 (2021).
- ¹⁰⁸F. Lipparini, L. Lagardère, G. Scalmani, B. Stamm, E. Cancès, Y. Maday, J.-P. Piquemal, M. J. Frisch, and B. Mennucci, “Quantum calculations in solution for large to very large molecules: A new linear scaling QM/continuum approach,” *J. Phys. Chem. Lett.* **5**, 953–958 (2014).
- ¹⁰⁹E. Cancès, Y. Maday, and B. Stamm, “Domain decomposition for implicit solvation models,” *J. Chem. Phys.* **139**, 054111 (2013).
- ¹¹⁰F. Lipparini, G. Scalmani, L. Lagardère, B. Stamm, E. Cancès, Y. Maday, J.-P. Piquemal, M. J. Frisch, and B. Mennucci, “Quantum, classical, and hybrid QM/MM calculations in solution: General implementation of the ddCOSMO linear scaling strategy,” *J. Chem. Phys.* **141**, 184108 (2014).
- ¹¹¹B. Stamm, L. Lagardère, G. Scalmani, P. Gatto, E. Cancès, J.-P. Piquemal, Y. Maday, B. Mennucci, and F. Lipparini, “How to make continuum solvation incredibly fast in a few simple steps: A practical guide to the domain

- decomposition paradigm for the conductor-like screening model," *Int. J. Quantum Chem.* **119**, e25669 (2019).
- ¹¹²F. Lipparini, B. Stamm, E. Cancès, Y. Maday, P. Gatto, J.-P. Piquemal, L. Lagardère, and B. Mennucci, see <https://github.com/filippolipparini/ddPCM>, doi: 10.5281/zenodo.1226641 for "A fast domain decomposition based implementation of the COSMO solvation model."
- ¹¹³M. Nottoli, B. Stamm, G. Scalmani, and F. Lipparini, "Quantum calculations in solution of energies, structures, and properties with a domain decomposition polarizable continuum model," *J. Chem. Theory Comput.* **15**, 6061–6073 (2019).
- ¹¹⁴C. J. Cramer and D. G. Truhlar, "A universal approach to solvation modeling," *Acc. Chem. Res.* **41**, 760–768 (2008).
- ¹¹⁵M. Orozco and F. J. Luque, "Theoretical methods for the description of the solvent effect in biomolecular systems," *Chem. Rev.* **100**, 4187–4226 (2000).
- ¹¹⁶C. Amovilli and B. Mennucci, "Self-consistent-field calculation of Pauli repulsion and dispersion contributions to the solvation free energy in the polarizable continuum model," *J. Phys. Chem. B* **101**, 1051–1057 (1997).
- ¹¹⁷L. Cupellini, C. Amovilli, and B. Mennucci, "Electronic excitations in nonpolar solvents: Can the polarizable continuum model accurately reproduce solvent effects?," *J. Phys. Chem. B* **119**, 8984–8991 (2015).
- ¹¹⁸A. V. Marenich, C. J. Cramer, and D. G. Truhlar, "Uniform treatment of solute–solvent dispersion in the ground and excited electronic states of the solute based on a solvation model with state-specific polarizability," *J. Chem. Theory Comput.* **9**, 3649–3659 (2013).
- ¹¹⁹C. Curutchet, L. Cupellini, J. Kongsted, S. Corni, L. Frediani, A. H. Steindal, C. A. Guido, G. Scalmani, and B. Mennucci, "Density-dependent formulation of dispersion–repulsion interactions in hybrid multiscale quantum/molecular mechanics (QM/MM) models," *J. Chem. Theory Comput.* **14**, 1671–1681 (2018).
- ¹²⁰A. Tkatchenko and M. Scheffler, "Accurate molecular van der Waals interactions from ground-state electron density and free-atom reference data," *Phys. Rev. Lett.* **102**, 073005 (2009).
- ¹²¹T. Giovannini, P. Lafosca, and C. Cappelli, "A general route to include Pauli repulsion and quantum dispersion effects in QM/MM approaches," *J. Chem. Theory Comput.* **13**, 4854–4870 (2017).
- ¹²²J. M. H. Olsen, C. Steinmann, K. Ruud, and J. Kongsted, "Polarizable density embedding: A new QM/QM/MM-based computational strategy," *J. Phys. Chem. A* **119**, 5344–5355 (2015).
- ¹²³P. Reinholdt, F. K. Jørgensen, J. Kongsted, and J. M. H. Olsen, "Polarizable density embedding for large biomolecular systems," *J. Chem. Theory Comput.* **16**, 5999–6006 (2020).
- ¹²⁴D. W. Zhang and J. Z. H. Zhang, "Molecular fractionation with conjugate caps for full quantum mechanical calculation of protein–molecule interaction energy," *J. Chem. Phys.* **119**, 3599–3605 (2003).
- ¹²⁵Q. Cui, T. Pal, and L. Xie, "Biomolecular QM/MM simulations: What are some of the 'burning issues'?", *J. Phys. Chem. B* **125**, 689–702 (2021).
- ¹²⁶P. Norman, K. Ruud, and T. Saue, *Principles and Practices of Molecular Properties: Theory, Modeling, and Simulations*, 1st ed. (John Wiley & Sons, Hoboken, NJ, 2018).
- ¹²⁷R. Cammi, B. Mennucci, and J. Tomasi, "On the calculation of local field factors for microscopic static hyperpolarizabilities of molecules in solution with the aid of quantum-mechanical methods," *J. Phys. Chem. A* **102**, 870–875 (1998).
- ¹²⁸S. Pipolo, R. Cammi, A. Rizzo, C. Cappelli, B. Mennucci, and J. Tomasi, "Cavity field effects within a polarizable continuum model of solvation: Application to the calculation of electronic circular dichroism spectra of *r*-(+)-3-methyl-cyclopentanone," *Int. J. Quantum Chem.* **111**, 826–838 (2011).
- ¹²⁹N. H. List, H. J. A. Jensen, and J. Kongsted, "Local electric fields and molecular properties in heterogeneous environments through polarizable embedding," *Phys. Chem. Chem. Phys.* **18**, 10070–10080 (2016).
- ¹³⁰N. H. List, J. M. H. Olsen, and J. Kongsted, "Excited states in large molecular systems through polarizable embedding," *Phys. Chem. Chem. Phys.* **18**, 20234–20250 (2016).
- ¹³¹R. C. Bernardi, M. C. Melo, and K. Schulten, "Enhanced sampling techniques in molecular dynamics simulations of biological systems," *Biochim. Biophys. Acta—Gen. Subj.* **1850**, 872–877 (2015).
- ¹³²C. Abrams and G. Bussi, "Enhanced sampling in molecular dynamics using metadynamics, replica-exchange, and temperature-acceleration," *Entropy* **16**, 163–199 (2013).
- ¹³³Y. Miao and J. A. McCammon, "Unconstrained enhanced sampling for free energy calculations of biomolecules: A review," *Mol. Simul.* **42**, 1046–1055 (2016).
- ¹³⁴M. Martinez, M.-P. Gaigeot, D. Borgis, and R. Vuilleumier, "Extracting effective normal modes from equilibrium dynamics at finite temperature," *J. Chem. Phys.* **125**, 144106 (2006).
- ¹³⁵M. Thomas, M. Brehm, R. Fligg, P. Vöhringer, and B. Kirchner, "Computing vibrational spectra from *ab initio* molecular dynamics," *Phys. Chem. Chem. Phys.* **15**, 6608–6622 (2013).
- ¹³⁶S. Mukamel, *Principles of Nonlinear Optical Spectroscopy* (Oxford University Press, New York, 1995).
- ¹³⁷S. Valleau, A. Eisfeld, and A. Aspuru-Guzik, "On the alternatives for bath correlators and spectral densities from mixed quantum-classical simulations," *J. Chem. Phys.* **137**, 224103 (2012).
- ¹³⁸S. Karsten, S. D. Ivanov, S. I. Bokarev, and O. Kühn, "Simulating vibronic spectra via Matsubara-like dynamics: Coping with the sign problem," *J. Chem. Phys.* **149**, 194103–194114 (2018).
- ¹³⁹D. Loco, S. Jurinovich, L. Cupellini, M. F. S. J. Menger, and B. Mennucci, "The modeling of the absorption lineshape for embedded molecules through a polarizable QM/MM approach," *Photochem. Photobiol. Sci.* **17**, 552–560 (2018).
- ¹⁴⁰D. Loco and L. Cupellini, "Modeling the absorption lineshape of embedded systems from molecular dynamics: A tutorial review," *Int. J. Quantum Chem.* **119**, e25726 (2019).
- ¹⁴¹M. Bondanza, L. Cupellini, F. Lipparini, and B. Mennucci, "The multiple roles of the protein in the photoactivation of orange carotenoid protein," *Chem* **6**, 187–203 (2020).
- ¹⁴²R. L. Leverenz, M. Sutter, A. Wilson, S. Gupta, A. Thurotte, C. Bourcier de Carbon, C. J. Petzold, C. Ralston, F. Perreau, D. Kirilovsky, and C. A. Kerfeld, "A 12 Å carotenoid translocation in a photoswitch associated with cyanobacterial photoprotection," *Science* **348**, 1463–1466 (2015).
- ¹⁴³L. Ridder, I. M. C. M. Rietjens, J. Vervoort, and A. J. Mulholland, "Quantum mechanical/molecular mechanical free energy simulations of the GlutathioneS-transferase (m1-1) reaction with phenanthrene 9,10-oxide," *J. Am. Chem. Soc.* **124**, 9926–9936 (2002).
- ¹⁴⁴A. Crespo, M. A. Martí, D. A. Estrin, and A. E. Roitberg, "Multiple-steering QM-MM calculation of the free energy profile in chorismate mutase," *J. Am. Chem. Soc.* **127**, 6940–6941 (2005).
- ¹⁴⁵H. M. Senn, S. Thiel, and W. Thiel, "Enzymatic hydroxylation in *p*-hydroxybenzoate hydroxylase: A case study for QM/MM molecular dynamics," *J. Chem. Theory Comput.* **1**, 494–505 (2005).
- ¹⁴⁶S. R. Billeter, C. F. W. Hanser, T. Z. Mordasini, M. Scholten, W. Thiel, and W. F. van Gunsteren, "Molecular dynamics study of oxygenation reactions catalysed by the enzyme *p*-hydroxybenzoate hydroxylase," *Phys. Chem. Chem. Phys.* **3**, 688–695 (2001).
- ¹⁴⁷J. E. Basner and S. D. Schwartz, "How enzyme dynamics helps catalyze a reaction in atomic detail: A transition path sampling study," *J. Am. Chem. Soc.* **127**, 13822–13831 (2005).
- ¹⁴⁸M. Nottoli, M. Bondanza, F. Lipparini, and B. Mennucci, "An enhanced sampling QM/AMOEBA approach: The case of the excited state intramolecular proton transfer in solvated 3-hydroxyflavone," *J. Chem. Phys.* **154**, 184107 (2021).
- ¹⁴⁹F. Ding, D. B. Lingerfelt, B. Mennucci, and X. Li, "Time-dependent non-equilibrium dielectric response in QM/continuum approaches," *J. Chem. Phys.* **142**, 034120 (2015).
- ¹⁵⁰S. Corni, S. Pipolo, and R. Cammi, "Equation of motion for the solvent polarization apparent charges in the polarizable continuum model: Application to real-time TDDFT," *J. Phys. Chem. A* **119**, 5405–5416 (2015).
- ¹⁵¹B. Lasorne, G. A. Worth, and M. A. Robb, "Excited-state dynamics," *Wiley Interdiscip. Rev.: Comput. Mol. Sci.* **1**, 460–475 (2011).
- ¹⁵²M. Persico and G. Granucci, "An overview of nonadiabatic dynamics simulations methods, with focus on the direct approach versus the fitting of potential energy surfaces," *Theor. Chem. Acc.* **133**, 1526–1528 (2014).

- ¹⁵³R. Crespo-Otero and M. Barbatti, "Recent advances and perspectives on non-adiabatic mixed quantum-classical dynamics," *Chem. Rev.* **118**, 7026–7068 (2018).
- ¹⁵⁴L. M. Ibele and B. F. E. Curchod, "A molecular perspective on Tully models for nonadiabatic dynamics," *Phys. Chem. Chem. Phys.* **22**, 15183–15196 (2020).
- ¹⁵⁵J. C. Tully and R. K. Preston, "Trajectory surface hopping approach to nonadiabatic molecular collisions: The reaction of H^+ with D_2 ," *J. Chem. Phys.* **55**, 562–572 (1971).
- ¹⁵⁶J. C. Tully, "Molecular dynamics with electronic transitions," *J. Chem. Phys.* **93**, 1061–1071 (1990).
- ¹⁵⁷M. Bondanza, M. Nottoli, L. Cupellini, F. Lipparini, and B. Mennucci, "Polarizable embedding QM/MM: The future gold standard for complex (bio)systems?," *Phys. Chem. Chem. Phys.* **22**, 14433–14448 (2020).
- ¹⁵⁸M. Nottoli, L. Cupellini, F. Lipparini, G. Granucci, and B. Mennucci, "Multiscale models for light-driven processes," *Ann. Rev. Phys. Chem.* **72**, 489–513 (2021).
- ¹⁵⁹B. W. J. Chen, L. Xu, and M. Mavrikakis, "Computational methods in heterogeneous catalysis," *Chem. Rev.* **121**, 1007–1048 (2021).
- ¹⁶⁰K. Mathew, V. S. C. Kolluru, S. Mula, S. N. Steinmann, and R. G. Hennig, "Implicit self-consistent electrolyte model in plane-wave density-functional theory," *J. Chem. Phys.* **151**, 234101 (2019).
- ¹⁶¹M. Saleheen and A. Heyden, "Liquid-phase modeling in heterogeneous catalysis," *ACS Catal.* **8**, 2188 (2018).
- ¹⁶²S. M. Morton, D. W. Silverstein, and L. Jensen, "Theoretical studies of plasmonics using electronic structure methods," *Chem. Rev.* **111**, 3962–3994 (2011).
- ¹⁶³J. Dong, Z. Zhang, H. Zheng, and M. Sun, "Recent progress on plasmon-enhanced fluorescence," *Nanophotonics* **4**, 472–490 (2015).
- ¹⁶⁴S. Schlücker, "Surface-enhanced Raman spectroscopy: Concepts and chemical applications," *Angew. Chem. (Int. Ed. Engl.)* **53**, 4756–4795 (2014).
- ¹⁶⁵A. B. Zrimsek, N. Chiang, M. Mattei, S. Zaleski, M. O. McAnally, C. T. Chapman, A.-I. Henry, G. C. Schatz, and R. P. Van Duyne, "Single-molecule chemistry with surface- and tip-enhanced Raman spectroscopy," *Chem. Rev.* **117**, 7583–7613 (2017).
- ¹⁶⁶C. Zhan, X.-J. Chen, J. Yi, J.-F. Li, D.-Y. Wu, and Z.-Q. Tian, "From plasmon-enhanced molecular spectroscopy to plasmon-mediated chemical reactions," *Nat. Rev. Chem.* **2**, 216–230 (2018).
- ¹⁶⁷J. L. Payton, S. M. Morton, J. E. Moore, and L. Jensen, "A hybrid atomistic electrostatics-quantum mechanical approach for simulating surface-enhanced Raman scattering," *Acc. Chem. Res.* **47**, 88–99 (2014).
- ¹⁶⁸Z. Rinkevicius, X. Li, J. A. R. Sandberg, K. V. Mikkelsen, and H. Ågren, "A hybrid density functional theory/molecular mechanics approach for linear response properties in heterogeneous environments," *J. Chem. Theory Comput.* **10**, 989–1003 (2014).
- ¹⁶⁹S. Mackowski, S. Wormke, A. J. Maier, T. H. P. Brotsudarmo, H. Harutyunyan, A. Hartschuh, A. O. Govorov, H. Scheer, and C. Brauchle, "Metal-enhanced fluorescence of chlorophylls in single light-harvesting complexes," *Nano Lett.* **8**, 558–564 (2008).
- ¹⁷⁰E. Wientjes, J. Renger, A. G. Curto, R. Cogdell, and N. F. van Hulst, "Strong antenna-enhanced fluorescence of a single light-harvesting complex shows photon antibunching," *Nat. Commun.* **5**, 4236 (2014).
- ¹⁷¹I. Kaminska, J. Bohlen, S. Mackowski, P. Tinnefeld, and G. P. Acuna, "Strong plasmonic enhancement of a single peridinin-chlorophyll a-protein complex on DNA origami-based optical antennas," *ACS Nano* **12**, 1650–1655 (2018).
- ¹⁷²F. Kyeeyune, J. L. Botha, B. van Heerden, P. Malý, R. van Grondelle, M. Diale, and T. P. J. Krüger, "Strong plasmonic fluorescence enhancement of individual plant light-harvesting complexes," *Nanoscale* **11**, 15139–15146 (2019).
- ¹⁷³C. Curutchet and B. Mennucci, "Quantum chemical studies of light harvesting," *Chem. Rev.* **117**, 294–343 (2017).
- ¹⁷⁴L. Cupellini, M. Bondanza, M. Nottoli, and B. Mennucci, "Successes & challenges in the atomistic modeling of light-harvesting and its photoregulation," *BBA—Bioenergetics* **1861**, 148049 (2020).
- ¹⁷⁵O. Andreussi, A. Biancardi, S. Corni, and B. Mennucci, "Plasmon-controlled light-harvesting: Design rules for biohybrid devices via multiscale modeling," *Nano Lett.* **13**, 4475–4484 (2013).
- ¹⁷⁶S. Caprasecca, C. A. Guido, and B. Mennucci, "Control of coherences and optical responses of pigment-protein complexes by plasmonic nanoantennae," *J. Phys. Chem. Lett.* **7**, 2189–2196 (2016).
- ¹⁷⁷S. Caprasecca, S. Corni, and B. Mennucci, "Shaping excitons in light-harvesting proteins through nanoplasmonics," *Chem. Sci.* **9**, 6219–6227 (2018).
- ¹⁷⁸Y.-J. Zhang, A. Khorshidi, G. Kastlunger, and A. A. Peterson, "The potential for machine learning in hybrid QM/MM calculations," *J. Chem. Phys.* **148**, 241740 (2018).
- ¹⁷⁹Y. Wang, J. M. Lamim Ribeiro, and P. Tiwary, "Machine learning approaches for analyzing and enhancing molecular dynamics simulations," *Curr. Opin. Struct. Biol.* **61**, 139–145 (2020).
- ¹⁸⁰J. Westermayr and P. Marquetand, "Machine learning for electronically excited states of molecules," *Chem. Rev.* **121**, 9873–9926 (2020).
- ¹⁸¹P. Friederich, F. Häse, J. Proppe, and A. Aspuru-Guzik, "Machine-learned potentials for next-generation matter simulations," *Nat. Mater.* **20**, 750–761 (2021).
- ¹⁸²O. T. Unke, S. Chmiela, H. E. Sauceda, M. Gastegger, I. Poltavsky, K. T. Schütt, A. Tkatchenko, and K.-R. Müller, "Machine learning force fields," *Chem. Rev.* **121**(16), 10142–10186 (2021).